048 KORTRAPPORT / BRIEF REPORT
NORSK POLARINSTITUTT · NORWEGIAN POLAR INSTITUTE 2018

Angelika H. H. Renner, Paul A. Dodd and Agneta Fransson

An assessment of MOSJ • The state of the marine climate system around Svalbard and Jan Mayen

MOSJ Miljøovervåking Svalbard og Jan Mayen

Kortrapport/Brief report nr 048

Angelika H. H. Renner, Paul A. Dodd and Agneta Fransson

An assessment of MOSJ • The state of the marine climate system around Svalbard and Jan Mayen

Addresses:

Angelika H. H. Renner
angelika.renner@hi.no
Institute of Marine Research
Tromsø Department
Fram Centre
P.O Box 6606, Langnes
9296 TROMSØ

Paul A. Dodd
paul.dodd@npolar.no
Norwegian Polar Institute
Fram Centre
P.O Box 6606, Langnes
9296 TROMSØ

Agneta Fransson
agneta.fransson@npolar.no
Norwegian Polar Institute
Fram Centre
P.O Box, Langnes
9296 TROMSØ

Norwegian Polar Institute, Fram Centre, NO-9296 Tromsø,
www.npolar.no, post@npolar.no

Techincal editor:	Gunn Sissel Jaklin, Norwegian Polar Institute (NPI)
Cover design:	Jan Roald, NPI
Cover photo:	Katrin Lindbäck, NPI. Kongsfjorden, Svalbard 2015.
Printed:	May 2018
ISBN:	978-82-7666-419-5 (printed edition)
ISBN:	978-82-7666-420-1 (digital edition)
ISSN:	0803-0421 (printed edition)
ISSN:	2464-1308 (digital edition)

Content

Summary

General status of the marine climate system components

Svalbard's climate is strongly influenced by the adjacent seas. Late-summer measurements collected over the last 52 years show that the temperature of warm Atlantic water flowing into the Arctic Ocean via in the West Spitsbergen Current has increased by 1.4 - 1.7 °C during the measurement period, equivalent to a rate of 0.27 – 0.33 °C per decade. The rate of warming has remained rather constant over the 52-year measurement period, excepting two warm (2005-2006, 2016-2017) anomalies and one cool (1998) anomaly. The West Spitsbergen current is an extension of the North Atlantic drift system and the trends observed in Eastern Fram Strait are largely due to increases in the temperature of water transported northwards from the sub-polar and sub-tropical Atlantic. Similar warming trends have been observed at other observatories along the North Atlantic Current system. The causes of this warming trend are the subject of ongoing research, and relevant factors include: variations in subtropical Atlantic water temperature; the rate of advection along the North Atlantic Current and the extent of wind-induced surface cooling on route.

Increased advection of heat has a strong impact on the ice cover around Svalbard, in the Barents Sea, and in Fram Strait. Sea ice extent and area have been decreasing drastically since the beginning of satellite observations in 1978, in places by as much as 12% per decade in winter and 21% per decade in summer. In particular the Barents Sea is now experiencing mostly ice-free summers. The sea ice cover in the Greenland Sea is continuously resupplied due to sea ice export from the central Arctic Ocean, however, here too extent is declining both in summer and in winter by 10% per decade. Long-term observations of sea ice thickness in Fram Strait reveal a thinning of over 50% during the period 2003-2014, particularly of multiyear ice, and a loss of old ice. North of Svalbard and in the Barents Sea, observations are too sporadic to determine long-term ice thickness trends, but time series from Hopen and various field campaigns suggest a thinning. Svalbard fjord fast ice has decreased both in extent and thickness, but longer time series from different regions around Svalbard are required for a better assessment.

The marine environment of many Svalbard fjords is strongly influenced by warm Atlantic water supplied by the West Spitsbergen Current or Barents Sea (at depth) and by glacial meltwater supplied from Svalbard glaciers (at the surface). Increased freshwater addition decreases aragonite and calcite saturation (Ω) and pH level, and increases the ocean acidification state to levels that are critical for calcium-carbonate forming marine organisms. Particularly sensitive to this change is the aragonite-shell forming pteropod *Limacina helicina*, living in fjords and areas that are already near critical limits ($\Omega < 1.4$) for calcification.

The Svalbard fjords Kongsfjorden and Tempelfjorden are experiencing increased ocean acidification state (OA) due to several factors: increased CO_2 due to anthropogenic CO_2 uptake in the Atlantic water outside the fjords, increased CO_2 due to more inflow of CO_2-rich Coastal Current water, and increased OA due to increased addition of glacial water. However, there are seasonal and inter-annual variability as well as biological CO_2 consumption that balance parts of the increased CO_2. In Storfjorden, OA

increases due to sinking of CO_2-equilibrated surface water during sea-ice and brine formation. CO_2-rich brine contributes to the relatively high CO_2 concentrations (low pH) at the bottom of the fjord.

Relative sea level, i.e. sea level relative to a coastal benchmark, is generally dropping in Svalbard by 2 to 4 mm/yr. However, large uncertainties are connected to the different drivers of sea level changes, which also act on different temporal and spatial scales. Svalbard and northern Norway still experience uplift due to glacial isostatic adjustment, which occurs over large spatial and long temporal scales and leads to vertical land motion of up to 1.4 mm/yr. More locally and on shorter time scales, processes related to glacier melt, groundwater processes and sediment compaction influence measurements and adjustment of coastal features. The current drop in sea level in Svalbard might therefore be a local phenomenon where processes specific to Svalbard counteract the global increase in sea level.

Evaluation of national environmental goals

The following national environmental goals that are particularly relevant to MOSJ, were formulated by the Norwegian government:

Goal 6.1: The current extent of wilderness-like areas in Svalbard will be retained, and biological and landscape diversity will be maintained virtually untouched by local human activity.

Goal 6.3: Environmental pressure from human activity and the risk of such pressure in the polar regions will be reduced.

Detailed indicators for goal 6.3 are still under development. The formulation of the environmental goals is rather broad which makes it difficult to assess progress towards meeting them.

In order to assess these goals we must first determine the extent to which human activity is responsible for the observed changes around Svalbard. Heat supplied by the West Spitsbergen Current has a large influence on Svalbard's climate, but until the causes of the warming trend observed in the West Spitsbergen Current are determined it is difficult to assess whether national environmental goals are or will be effective in limiting the observed changes.

The decline in Arctic sea ice is mostly driven by large-scale atmospheric and oceanic factors, including the observed warming in both atmosphere and ocean. Attribution of climatic changes to human activity has been confirmed (IPCC, 2013), and thus the influence of human activity on large-scale atmospheric and oceanic circulation and the Arctic sea ice cover. However, further studies are needed to assess the potential impact of local activity on the local to regional sea ice cover, ranging from the fast ice in Svalbard fjords to the pack ice in the Barents Sea and in Fram Strait.

For the monitoring of the carbonate chemistry and OA state in Svalbard fjords (Kongsfjorden and Rijpfjorden) in summer (in July/August 2013-2017) and in Fram Strait (in August/September 2012-2017), the national goals have mostly been met. These goals are met with help of the Fram Centre OA flagship project. Also regarding the collection of pteropods in Kongsfjorden and Rijpfjorden part of the goals have been met. However, there is still a need for long-term observations and seasonal data on the OA state and development of the methods for sampling of pteropods and analyses of the aragonite shell (Manno et al. 2017).

Human activity is contributing in different ways to global sea level rise, but might also influence relative sea level changes in Svalbard due to local processes. An assessment of the factors influencing relative sea level at the Svalbard tide gauges is needed, followed by an assessment of the human impact on these factors before we can draw detailed conclusions with respect to the national environmental goals. Pressure from human activity is clearly felt in the MOSJ region, however, this activity is largely taking place outside the polar regions. To meet the national environmental goals, actions therefore need to take place both locally in Svalbard and the surrounding seas, and on mainland Norway and beyond.

Recommendations

The West Spitsbergen Current is one of the largest sources of heat to the Arctic and further research is required to determine which processes affect the amount of heat supplied to the Arctic via this route. The International scientific community is actively investigating the problem and Norway contributes to the international effort by providing observations of the properties of the West Spitsbergen Current in Fram Strait. The present observing system in Eastern Fram Strait consists of annually repeated sections where salinity and temperature are measured using a shipboard CTD (conductivity, temperature and depth) sonde. These sections effectively monitor the summer situation. The situation in winter is much less well observed, and it is in winter that oceanic heat provided by the West Spitsbergen Current has the largest influence of sea ice extent and air temperatures around Svalbard. Since 1997 the international scientific community has maintained an array of moorings that monitor the hydrographic properties of the West Spitsbergen Current, which is planned to continue in the long term. While these moored instruments provide year-round measurements at several depths and locations, they do not observe the surface layer, which interacts directly with the atmosphere and sea ice cover and which is likely to change most rapidly. Winter CTD measurements would complement the moored instruments by providing measurements from the surface layer.

Sea ice thickness in Fram Strait is covered well all-year round by the moored array, however, comparable observations are missing for the areas north of Svalbard and in the Barents Sea, where only sporadic campaigns exist. There is room for improvement in the spatial, temporal and methodological consistency of sea ice thickness measurements in these areas. It would be beneficial to implement a program of regularly repeated sea ice thickness measurements in key locations, using a consistent approach. Large-scale ice extent and area are covered well through satellite observations, but near the coast, reliable drift and fast-ice extent observations are missing. With the development of new satellite sensors and algorithms (e.g. from CryoSat-2, SMOS, and the Sentinel missions), a monitoring system using those should be established. In situ observations are critical for ground-truthing and measurements of the physical properties of the sea ice. More resources are required though to maintain these observations and process and publish the data.

Before 2012, there were almost no observations of the carbonate chemistry and ocean acidification state (OA) in Svalbard fjords, apart from a mesocosm study in Kongsfjorden in 2008-2009 during the European Project on Ocean Acidification (EPOCA) project. In Fram Strait (at 79° N), there were few ship-based observations of the carbonate chemistry (e.g. Jeanson et al. 2008; 2010). However, time-series in the Fram Strait area at 79° N were lacking, in particular on the western side, in the East Greenland

Current (EGC), where the physical-chemical properties in the Arctic Ocean outflow water can be observed (Chierici et al. 2013). Further south, in the in Greenland Sea along 75° N there were several studies on the carbonate chemistry during European projects such as the European Subpolar Ocean Programme (ESOP; CARINA/CDIAC data bases; references e.g. Anderson et al. 1999; 2000; Chierici et al. 1999; Skjelvan et al. 1999; Olsen et al. 2003; 2009; 2010; Jutterström et al. 2008; Nondal et al. 2009). With the Fram Centre Ocean Acidification flagship and collaboration between Norwegian Polar Institute (NPI) and Institute of Marine Research (IMR), a new field-sampling project was initiated in 2011 with extensive water-sample collection and analyses of the carbonate chemistry in Fram Strait (79° N) and around Svalbard. However, there are still knowledge and data gaps in inter-annual and seasonal carbonate chemistry (ocean acidification) from Svalbard fjords, in particular in winter. These gaps include the distribution and effect of ocean acidification on pteropods *Limacina helicina* in other seasons than summer (study life cycle) and in other Svalbard fjords than Kongsfjorden, Tempelfjorden, Storfjorden and Rijpfjorden.

To fill some seasonal and inter-annual data gaps on carbonate chemistry and ocean acidification, we recommend adding CO_2 and pH sensors to existing and planned moorings in Svalbard fjords, Fram Strait and north of Svalbard. We also recommend continuation of already started time-series in Fram Strait and Kongsfjorden but also new time-series for long-time monitoring in other fjords. In 2016-2017, a CO_2 sensor recorded seasonal data in CO_2 Kongsfjorden. For chemical indicators of ocean acidification, we recommend calcium carbonate (e.g. aragonite saturation, Ω), pH and pCO_2. Sampling of pteropods *Limacina helicina* has been taken place in Kongsfjorden and Rijpfjorden from 2013-2016 but there is a need for sampling during other seasons and in other Svalbard fjords as well. There is also a need for method development and study of the effect of OA on pteropods.

Currently, two tide gauges exist in Svalbard whereas on mainland Norway, a network of tide gauges is maintained. The observations from the tide gauges in Barentsburg, Tromsø and Vardø are currently active indicators for MOSJ. The choice of these tide gauges should be evaluated as the monitoring could benefit from including other locations as well, e.g. Ny-Ålesund and Hammerfest. A recent report analysed sea level change along the Norwegian coast but omitted Svalbard. It would be a valuable study to review past, current and projected changes for Svalbard as well.

The set of indicators currently active and implemented in MOSJ are useful for an assessment of the marine environment around Svalbard, however, there are clear deficits. While some indicators are well established and defined (e.g. temperature and salinity in the West Spitsbergen Current), other areas completely lack established indicators (e.g. Ocean Acidification). There is an urgent need for better balance in the indicator set and broader coverage of different aspects of the marine environment. Similarly, standards of the indicators should be more uniform regarding availability of data and temporal coverage.

Norsk sammendrag

Klimaet på Svalbard er sterkt påvirket av havområdene utenfor. Målinger på sensommeren over de siste 52 årene viser at temperaturen i atlantisk havvann som strømmer inn i Polhavet via Vest-Spitsbergenstrømmen har økt med 1,4-1,7 °C i løpet av måleperioden. Det tilsvarer en økning på 0,27-0,33 °C per tiår. Med unntak av to varme avviksperioder i 2005-2006 og 2016-2017, og et kaldt avvik i 1998, har frekvensen av oppvarmingen vært forholdsvis konstant over måleperioden. Årsakene til trenden er gjenstand for pågående forskning, og relevante faktorer inkluderer: Variasjoner i subtropisk atlantisk vanntemperatur, frekvensen av vanntransport nordover, og omfanget av vind-indusert overflatekjøling.

Økt transport av varmt havvann har sterk innvirkning på havisen rundt Svalbard, i Barentshavet og i Framstredet. Utbredelsen av havis har sunket drastisk siden satellittbaserte målinger startet i 1978. I noen områder har reduksjonen av havis vært på så mye som 12 % per tiår om vinteren, og 21 % per tiår om sommeren. I særdeleshet er Barentshavet nå stort sett isfritt om sommeren. Havisen i Grønlandshavet blir kontinuerlig erstattet med is transportert ned fra Polhavet der det også her er registrert en nedgang i isutbredelse tilsvarende 10 % per tiår. Langtidsobservasjoner i Framstredet av istykkelse har vist en tynning på vel 50 % i perioden 2003-2014, og særlig gjelder dette for is med en alder på flere år. Nord for Svalbard og i Barentshavet er observasjonene for sporadiske for å beregne langsiktige trender for endring i istykkelse og alder, men en tidsserie fra Hopen og sporadiske observasjoner tyder på at havisen blir tynnere.

Det marine miljøet i mange fjorder på Svalbard og i Barentshavet er sterkt påvirket av varmt atlantisk vann og av smeltevann fra isbreene på Svalbard. Økt ferskvann i de øvre vannmassene reduserer konsentrasjonen av kalsium-karbonat (Ω) i form av aragonitt og kalsitt, og endrer vannets surhetsgrad (pH nivå) til et nivå som har negativ effekt på overlevelse for en del kalkholdige marine organismer. Spesielt følsomme for denne endringen er vingesneglen (*Limacina helicina*). Nyere undersøkelser viser at miljøet i fjordene på Svalbard nærmer seg en kritiske grenser ($\Omega < 1.4$) for denne artens evne til å danne kalkskall.

Kongsfjorden og Tempelfjorden på Svalbard forsures av flere forhold: Innstrømning av forsuret havvann fra menneskeskapte CO_2-kilder via Vest-Spitsbergenstrømmen, økt innstrømning av CO_2-rikt havvann fra kyststrømmene rundt Svalbard, og økt avrenning fra isbreene. I Storfjorden øker surhetsgraden som følge av avrenning fra land og ved dannelse av havis og påfølgende økning i vannets saltholdighet. CO_2-rikt havvann med høy saltholdighet bidrar vesentlig til den forsuringen som er registrert i bunnen av fjorden på øygruppen.

Det relative havnivået, langs kysten av Svalbard (dvs. havnivå relativt til et referansepunkt på kysten) synker 2 til 4 millimeter per år. Drivkreftene bak dette er usikre, men landområdene på Svalbard og i Nord-Norge hever seg fortsatt etter siste istid med en hastighet på 1,4 millimeter per år. Mer lokalt, og på kortere tidsskala, er landhevningen forårsaket av bresmelting, grunnvann prosesser, og komprimering av sedimenter. Det synkende havnivået vil kunne motvirke effekter på øygruppen som følge av en generell økning av havnivået.

Evaluering av de to nasjonale miljømålene som gjelder for Svalbard, viser at målene er for altomfattende og generelle til å gjøre en konkret evaluering i relasjon til denne rapportens tema. Nedgangen i isdekket i Polhavet er hovedsakelig drevet av oseanografiske og atmosfæriske faktorer, og påvirkes nå av en

observert oppvarming av atmosfæren og havmassene som ifølge FNs klimapanel knyttes til global oppvarming forårsaket av menneskelig aktivitet. Oppvarming av vannmassene rundt Svalbard er hovedsakelig forårsaket av variasjoner i innstrømning av varmt atlantisk havvann. Fordi årsakene til økning i vanntemperaturen fortsatt er uklar, er det vanskelig å vurdere om eventuelle nasjonale tiltak har eller vil ha effekt på de observerte endringene i havtemperaturen, havisen og havforsuring som registreres rundt øygruppen.

Med bakgrunn i denne utredningen anbefales følgende:

- Norge bør fortsette å bidra inn i den internasjonale forskningen på Vest-Spitsbergenstrømmen ved å opprettholde forskningsaktiviteten i Framstredet og rundt Svalbard, og det er behov for å øke innsatsen om vinteren. CTD målinger (konduktivitet, temperatur og dyp) om vinteren vil utfylle datainnhentingen fra fortøyde måleinstrumenter med data fra havoverflaten.
- Mens graden av målinger av istykkelse i Framstredet er tilfredsstillende, er det bare sporadiske målinger i havområdene nord for Svalbard og i Barentshavet. Det burde igangsettes et program for regelmessige målinger i havisen også i disse områdene.
- Storskala isutbredelse er godt dekket igjennom satellittobservasjoner, men pålitelige målinger av havis nær kysten mangler og bør etableres. Feltobservasjoner av havis er avgjørende for å innhente grunnleggende kunnskap om isens fysiske egenskaper, og det er derfor nødvendig å styrke dagens observasjoner i felt.
- Det er få data på havforsuring i fjordene på Svalbard i tidsrommet før 2012. Norsk Polarinstitutt og Havforskningsinstituttet har etter 2012 etablert et prosjekt med omfattende vannprøvetaking og analyser av karbonat-kjemi i Framstredet og rundt Svalbard, men mangler et opplegg for vinterobservasjoner. Dette prosjektet bør videreføres og suppleres med vinterobservasjoner, og inkludere effektstudier av havforsuring på vingesneglens (*Limacina helicina*) livssyklus gjennom hele året i flere fjorder på Svalbard, for å finne ut om vingesnegl er en god indikator for havforsuring. Andre marine organismer må også vurderes.
- For å fylle sesongmessige og mellomårlige kunnskapshull på karbonatkjemi og havforsuring, anbefales det å legge CO_2 og pH-sensorer til eksisterende og planlagte fortøyninger av måleinstrumenter i fjorder på Svalbard, nord for Svalbard og i Framstredet. Videre bør tidsseriene i Framstredet og Kongsfjorden videreføres, og det bør etableres langtidsovervåking også i andre fjorder på Svalbard. Når det gjelder kjemiske indikatorer knyttet til havforsuring anbefales overvåkning av kalsium-karbonat (f.eks. av aragonitt metning, Ω), pH og pCO_2.
- Målinger av havnivå i Barentsburg, Tromsø og Vardø blir per i dag rapportert i MOSJ. Det bør gjøres en vurdering av nytteverdien av å supplere med målinger i Ny-Ålesund og Hammerfest. En fersk rapport analyserte havnivå endringer langs den norske kysten, men unnlot Svalbard. Det vil være en verdifull studie for å gjennomgå tidligere, nåværende og anslåtte endringer på Svalbard.
- Antall indikatorer som for tiden er aktive og implementert i MOSJ er nyttige for en vurdering av havmiljøet rundt Svalbard, men det er tydelige mangler. Mens enkelte indikatorer er godt etablert og definert (for eksempel temperatur og saltholdighet i Vest-Spitsbergenstrømmen), mangler andre indikatorer, som for eksempel havforsuring. Det er et presserende behov for bedre balanse i indikatorsettet og bredere dekning av ulike aspekter av havmiljøet. Tilsvarende bør standardene for indikatorene være mer enhetlige med hensyn til tilgjengeligheten av data og tidsmessig dekning.

1. Introduction

The Environmental Monitoring of Svalbard and Jan Mayen (MOSJ) is an umbrella programme that collects and interprets relevant data series of the environment in the arctic territories of Svalbard and Jan Mayen. The present report is the interpretation of the indicator set with respect to the marine environment and focuses on the following key indicators:

- The extent and thickness of sea ice around Svalbard, in Fram Strait, and in the Barents Sea;
- The temperature and salinity of water supplied to the marine environment around Svalbard via the West Spitsbergen Current in Fram Strait;
- Ocean acidification in western Svalbard fjords and in Fram Strait;
- Local changes in sea level.

The objective of the report is twofold. Firstly, the report assesses the status of the marine physical and chemical (biogeochemical) environment as revealed by each indicator and evaluates the relevance of each individual indicator together with the monitoring design. Secondly, the report evaluates whether the national environmental goals have been achieved. Several of the above mentioned indicators are developed, defined, and monitored through MOSJ, including: sea ice extent in the Barents Sea and in the Greenland Sea (Fram Strait); sea ice thickness in Fram Strait; temperature, salinity and freshwater transport through Fram Strait; and sea level in Barentsburg, Tromsø and Vardø. This set of indicators developed under MOSJ build the base for the assessment. However, indicators are not developed yet for monitoring of Svalbard fjord sea ice cover and hydrography, and ocean acidification. Therefore, additional data, studies, and publications are used were relevant and available. Gaps in the current monitoring are identified and recommendations are given for future improvement of the monitoring programme.

2. Climate indicators – current state and trends for central components of the marine climate system

2.1 Sea ice extent & thickness

2.1.1 Introduction

Arctic sea ice is a major component of the global climate system and an indicator for ongoing climate change. Both sea ice extent and thickness have declined drastically over the past few decades (e.g. Meier et al. 2014) as a consequence of anthropogenic global warming (IPCC, 2013). The decrease in Arctic sea ice extent has been most pronounced in summer (13.3% per decade, Fig. 1; Fetterer et al. 2016), but is significant also in winter (2.7% per decade). Thickness has decreased due to loss of old, thick ice, and in general, the Arctic sea ice cover now consists of on average younger ice.

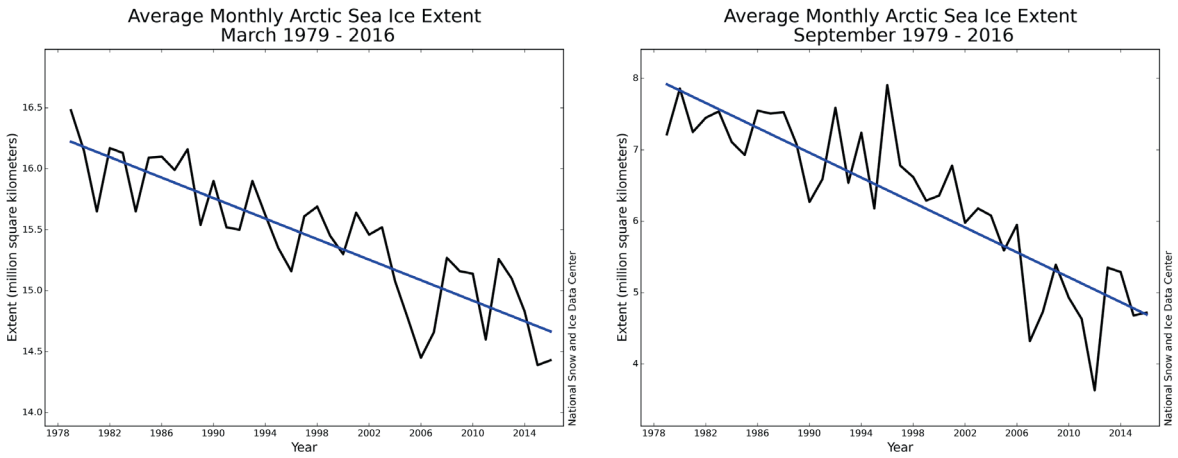

***Figure 1**: Arctic maximum (left) and minimum (right) sea ice extent (black line) and trend (blue line). Source: National Snow and Ice Data Center (NSIDC) Arctic Sea Ice News.*

The MOSJ area includes regions with very different sea ice characteristics (Fig. 2). Svalbard fjords differ depending on whether they are under the influence of mostly Atlantic-derived waters on the west and northwest coast of Svalbard, or more polar waters on the east coast. The Barents Sea is dominated by first and second-year ice, formed locally or advected in from the north whereas the Fram Strait ice cover includes old ice that is moving out of the central Arctic Ocean. In all regions, however, the ice cover is shrinking, with significant impact on the local climate, ecosystems, and on human activities.

Sea ice around Svalbard. Photo: Angelika H.H. Renner, 2011.

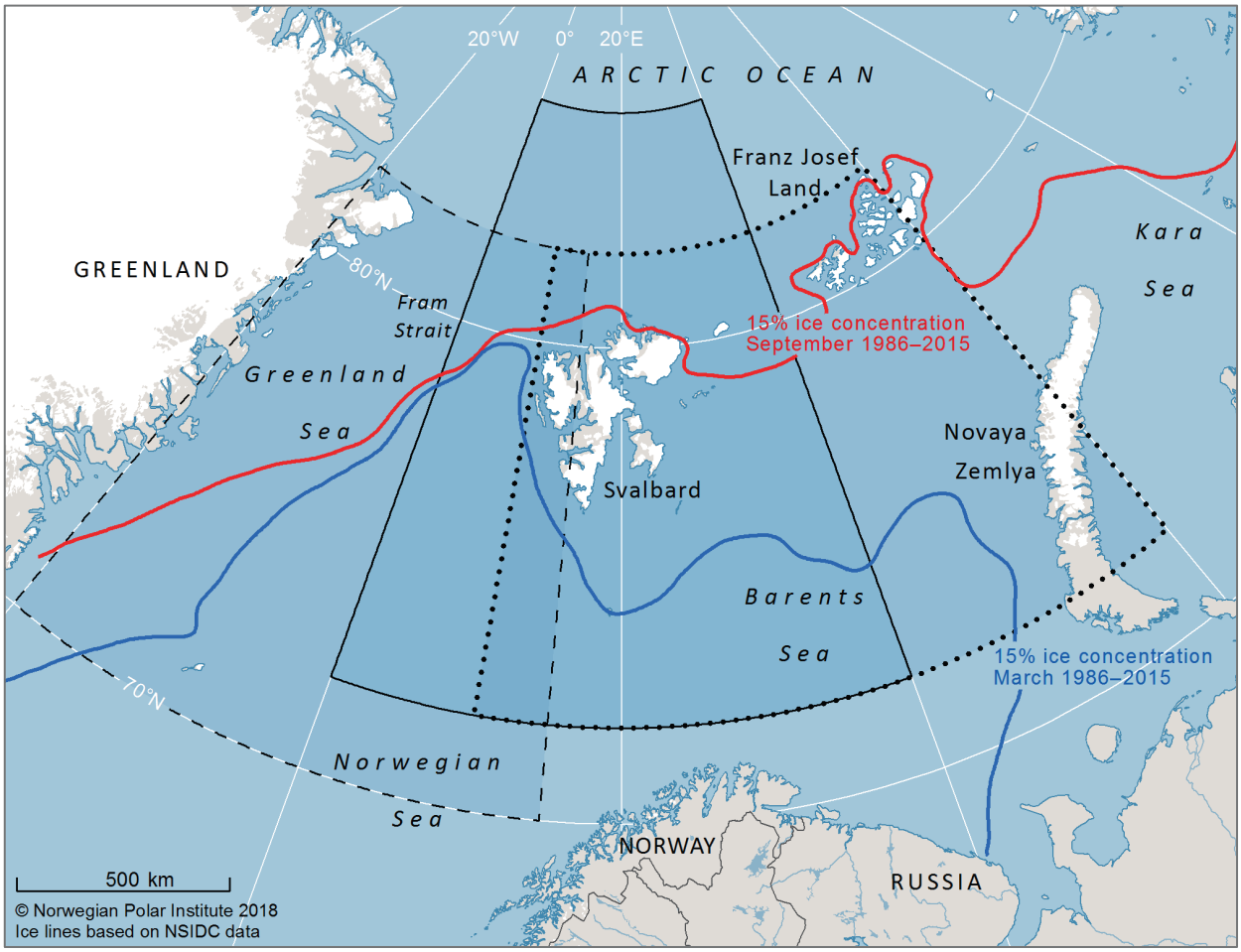

Figure 2: *Map of the extended region around Svalbard and Jan Mayen. The climatological average location of the sea ice edge (defined as 15% sea ice concentration contour) is indicated in red for September and in blue for March. Solid, dashed and dotted black lines denote the limits of the regions used to calculate sea ice area around Svalbard, sea ice extent in the Greenland Sea, and sea ice extent in the Barents Sea, respectively.*

2.1.2 Monitoring method

Official indicators within MOSJ include sea ice extent in the Greenland Sea and the Barents Sea, sea ice thickness and flux in Fram Strait, fast ice extent and thickness in Kongsfjorden, and fast ice thickness in Storfjorden (Inglefieldbukta) and at Hopen. Indicators in the Greenland Sea, Fram Strait, and Barents Sea are developed and available from MOSJ, Svalbard fjord indicators and Hopen are yet to be developed. For this report, we also consider other sources that are relevant for an assessment of the state of the sea ice in the MOSJ region.

Sea ice extent and area are being monitored using satellite data from various sources (sea ice extent is the areal extent of the region covered by at least 15 % sea ice where as sea ice area is only the ice covered part, i.e. sea ice extent x sea ice concentration). Arctic-wide datasets are derived from passive microwave satellite sensors by various international groups. In Norway, the Norwegian Polar Institute extract sea ice extent in the Barents Sea and in the Greenland Sea for MOSJ, and methods are described on the MOSJ webpages. The Barents Sea area is defined as a box between 72 – 82° N and 10 – 60° E.

The Greenland Sea is limited to 70 – 82° N, 20° W – 15° E (Figure 2.). The Norwegian Ice Service at the Norwegian Meteorological Institute produces operational daily ice charts for the European Arctic including Svalbard using satellite data from SAR, visual and infrared data. A Svalbard daily sea ice area index is derived from these charts for the area around Svalbard (0 – 40° E, 72 – 85° N).

Fjord ice monitoring is more difficult to achieve since in the case of passive microwave sensors, horizontal resolution is not sufficient, and SAR images are difficult to interpret for fast ice. NPI is using visual observations to map the development of fast ice extent in Kongsfjorden (Gerland & Renner, 2007). SAR satellite data have been used for a study on the sea ice cover in Hornsund and Isfjord (Muckenhuber et al. 2016).

In recent years, several satellites and algorithms have been developed to observe sea ice thickness from space which now cover both thin and thick sea ice throughout most of the year (e.g. ICE-Sat, CryoSat-2, SMOS). However, time series are still too short for monitoring purposes. Instead, in situ observations are necessary, both from fieldwork and autonomous platforms such as moorings. Sea ice thickness monitoring is done throughout the year in Fram Strait using mooring upward looking sonars deployed by NPI (Hansen et al. 2013). Around Svalbard, ice thickness monitoring is more patchy: NPI personnel at the station in Ny-Ålesund are measuring thickness when possible on the fast ice in Kongsfjorden (Gerland & Renner 2007), and annual field trips are conducted to Inglefieldbukta on the west coast of Storfjorden, east Spitsbergen. Fast ice at Hopen is monitored by personnel from the met.no station (Gerland et al. 2008). Airborne surveys in Fram Strait, Svalbard fjords, and north of Svalbard and in the Barents Sea take place irregularly but are invaluable to provide a larger scale overview (e.g. Renner et al. 2013; Renner et al. 2014; King et al. 2017). Recent developments of new sea ice thickness retrievals from satellite are promising for future large scale monitoring.

2.1.3 Svalbard fjord fast ice

Monitoring of fjord fast ice is very limited. Results from NPI's monitoring in Kongsfjorden were discussed already in Hansen (2010). While the monitoring is being continued, an updated time series is forthcoming and has been submitted for publication (S. Gerland, pers. comm.). Results from Inglefieldbukta in Storfjorden are also in preparation. They will be highly valuable to assess the situation on the east coast of Spitsbergen where time series are lacking.

Recently, Muckenhuber et al. (2016) used satellite remote sensing data to investigate fast ice coverage in Isfjorden and Hornsund on the west coast of Spitsbergen over the period 2000-2014. While studies looking at regionally limited locations exist in both fjords (e.g. Kruszewski 2012; Zhuravskiy et al. 2012), Muckenhuber et al. (2016) investigate the ice cover over the entire area of both fjords. They find the fast ice extent to be connected to heat content in the fjords, which is related the amount of warm Atlantic Water from the West Spitsbergen Current entering the fjord. They hypothesize that both large-scale forcing related to the strength and heat content of the West Spitsbergen Current and large-scale wind patterns as well as local forcing related to air temperature, fast ice extent and new ice formation drive the fast ice development in both Isfjorden and Hornsund. The time series exhibits a large degree of variability, and is not long enough to reliably estimate any trends in the ice cover. Muckenhuber et al. (2016) find, however, a distinct shift towards reduced ice coverage in 2006 in both fjords and suggest a causal link to increased temperatures in the water column in autumn.

2.1.4 Svalbard sea ice area

Sea ice around Svalbard is heavily influenced not only by local ice formation and melt, but also by advection of sea ice into the region through both currents and winds. While there is an annual cycle, it is fairly variable, and the timing of the annual minimum and maximum extent and area are not as predictable as for the Arctic as a whole. Using the Svalbard daily sea ice area index from the Norwegian Ice Service (N. Hughes, pers. comm. 2017), we calculated time series of monthly anomalies by calculating monthly mean ice area and substracting monthly climatological values. The time series starts in January 1967 and is shown in Fig. 3.

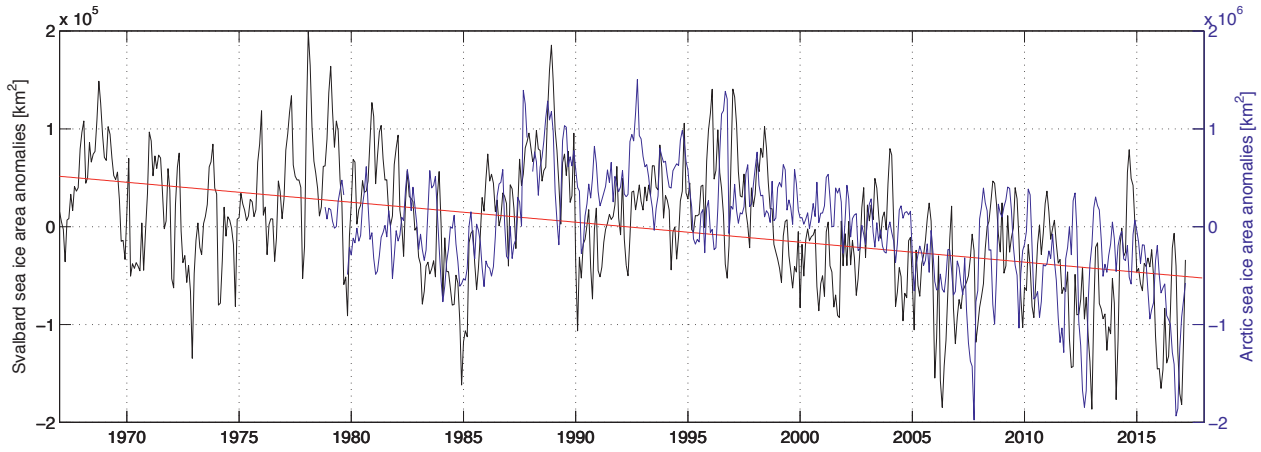

***Figure 3**: Monthly sea ice area (extent x concentration) anomalies Arctic-wide (blue), around Svalbard (black) and Svalbard ice area trend for 1967-2016 (red). Derived from: Svalbard daily sea ice area index, Norwegian Ice Service, 2017, and NSIDC sea ice index, version 2 (Fetterer et al. 2016).*

There is significant interannual variability that does not necessarily reflect the Arctic-wide variability but instead is likely due to regional processes. Overall, sea ice area around Svalbard has been decreasing by 2107 km^2/yr over the period 1967-2016. This decrease has been pronounced on the west Svalbard shelf, but a proper analysis of regional trends in different parts of the archipelago (e.g. north and east of Spitsbergen and Svalbard) and during different seasons is missing.

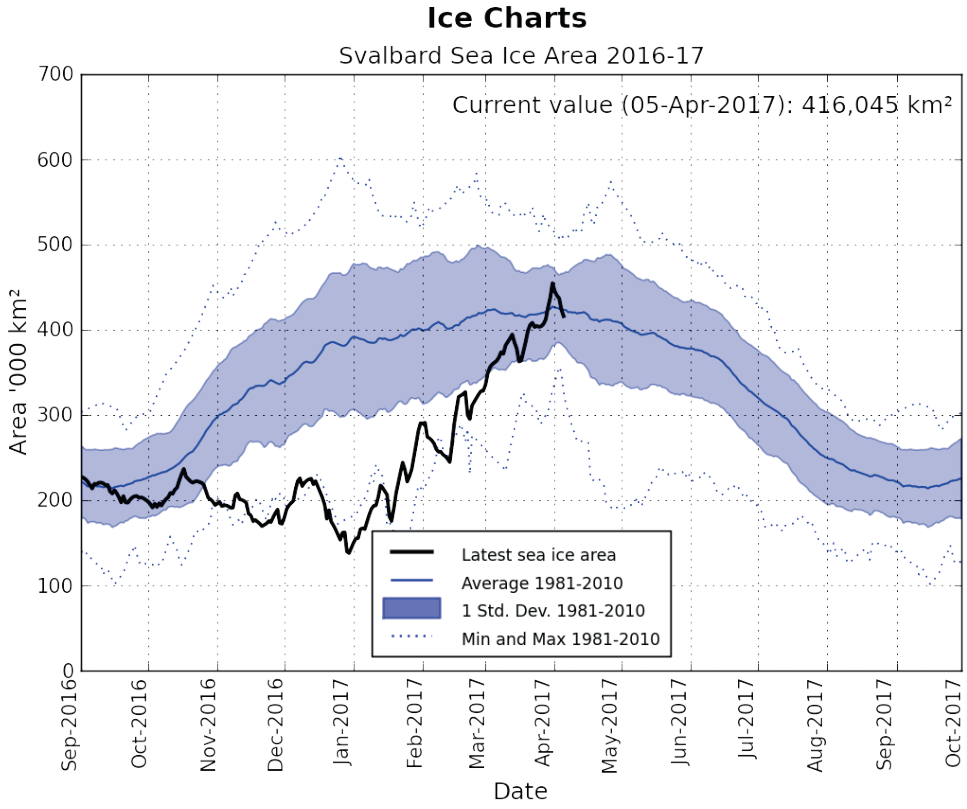

***Figure 4**: Current sea ice area around Svalbard, derived from ice charts, in comparison with climatology. Source: Ice Service, Norwegian Meteorological Institute.*

The development of ice growth during the 2016/2017 winter was rather unusual (Fig. 4). A very slow freeze up with several prolonged melt periods even in winter was followed by fast freezing in January to March. This is consistent with observations in the Barents Sea and other Arctic shelf seas, leading to the lowest March extent during 1979-2017 in the Arctic Ocean. The sea ice area around Svalbard has, after a very late freeze onset reached close to climatological values in April.

2.1.5 Barents Sea & Greenland Sea sea ice extent

The sea ice extent in the Barents Sea and in the Greenland Sea as monitored by MOSJ show a clear decline over the observation period (Fig. 5). Since the last report (Fauchald et al. 2014), the negative trend has accelerated in both regions and both in April and in September (Table 1). The Barents Sea experiences the fastest loss and has even been nearly ice-free at the end of summer in three of the last six years. Interestingly, the Svalbard sea ice area introduced and discussed in the previous section is decreasing at a slower rate than the ice extent in the neighbouring regions. This might be due to local processes around the islands and in the fjords, or a change in the open water fraction leading to a larger impact on sea ice extent. Regardless of whether ice extent or ice area is considered, the decrease in winter ice cover in the Greenland Sea, in the Barents Sea, and around Svalbard is occurring at a faster rate than the overall Arctic sea ice decline, whereas in summer, only the Barents Sea ice cover is retreating faster than the Arctic-wide average.

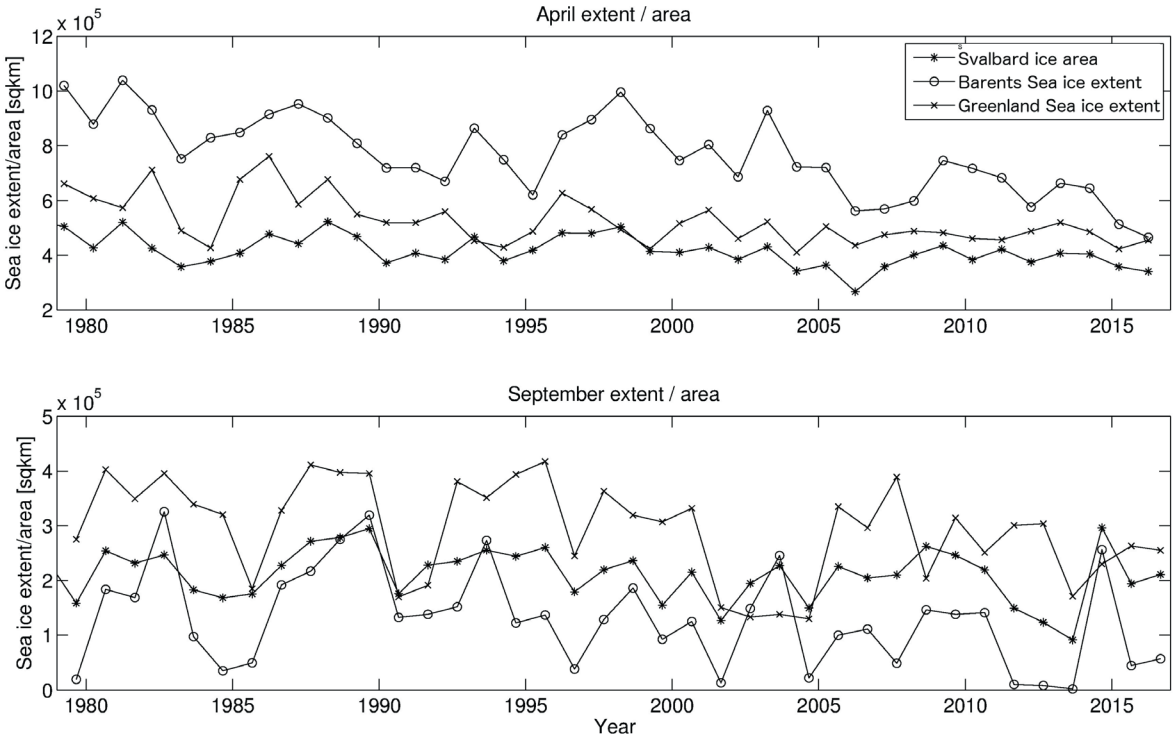

***Figure 5**: Seasonal sea ice extent in the Barents Sea, and in the Greenland Sea from passive microwave, and sea ice area around Svalbard from ice charts.*

***Table 1**: Trends in sea ice extent/area for the period 1979-2016 in April and September.*

	April*			September		
	mean [km^2]	trend [km^2/yr]	trend [%/decade]	mean	trend [km^2/yr]	trend [%/decade]
Svalbard sea ice area	414.678	-2324	-5.6	211.224	-937	-4.4
Barents Sea sea ice extent	767.566	-9447	-12.3	128.964	-2720	-21.1
Greenland Sea sea ice extent	525.000	-4752	-9.1	293.043	-3053	-10.4
Arctic-wide sea ice extent			-2.7 (March trend)			-13.3

* The maximum extent in the Barents Sea occurs usually in April, whereas it is more variable in the Greenland Sea; the MOSJ indicator uses April extent for both. The Arctic-wide maximum occurs in March.

The loss of sea ice in the MOSJ region has recently been discussed in several publications. Onarheim et al. (2014) showed that the decrease of the sea ice north of Svalbard is not restricted to the summer ice cover, but winter ice extent is declining as well. They argue that the long-term loss is driven by increased advection of oceanic heat with the Atlantic Water entering the Arctic, but suggest also that interannual variability is influenced by local wind. Pavlova et al. (2014) found that wind plays a major role for the sea

ice extent in the Barents Sea by influencing both the inflow of Atlantic Water and redistributing sea ice in the region. Herbaut et al. (2015), however, suggest that the ice cover does not behave uniformly across the entire Barents Sea, but that instead, the northern and the eastern parts of the Barents Sea react differently to wind and oceanic forcing. Their results show a stronger response of the northern Barents Sea ice cover to Atlantic Water inflow, whereas in the east, wind effects dominate. While it often is assumed that changes in ocean heat govern variability of the ice cover on longer timescales, Lien et al. (2017) find ocean forcing also to contribute to seasonal variability through atmospherically driven heat transport anomalies on monthly and seasonal time scales, e.g. changing the timing of winter freezeup.

The Greenland Sea ice extent is related to dynamic and thermodynamic processes in the central Arctic basin as it includes Fram Strait, which is the main outflow gateway from the Arctic. In addition, local ice formation and melt contribute to ice extent variability in the Greenland Sea. The sea ice cover in Fram Strait integrates a variety of signals from the central Arctic, it is therefore not straightforward to relate Fram Strait and subsequently Greenland Sea sea ice characteristics to those observed elsewhere. Renner et al. (2014) did not find a relationship between Fram Strait and Arctic-wide sea ice extent. Large variability in ice area export makes the assessment of potential trends difficult (e.g. Spreen et al. 2009; Smedsrud et al. 2011; Kwok et al. 2013; Krumpen et al. 2016). Most recently, Smedsrud et al. (2017) present a 80-year time series of ice area export through Fram Strait covering 1935-2014, which does not show a significant trend over the full period, but a potential increase over the last 35 years.

2.1.6 Fram Strait sea ice thickness

The development of sea ice thickness across Fram Strait has been discussed in previous reports (Hansen 2010; Fauchald et al. 2014) based on results presented by Hansen et al. (2013). They found a strong decline in multiyear ice thickness, which was confirmed using in situ and airborne observations in the same region by Renner et al. (2014). Krumpen et al. (2016) present observations further north in Fram Strait with the same results – thinning and decrease of multiyear ice, as well as a decrease in ice age.

Hansen et al. (2014) report a decrease of the modal ice thickness in the upward looking sonar record. They attribute this decrease to the thinning of first-year ice. Ice thicker than 5 m (i.e. heavily deformed ice) was lost however. These two processes lead to simultaneously increasing the fraction of thin ice and reducing the fraction of thick ice in the ice thickness distribution, thus reducing the modal ice thickness. Hansen et al. (2015) find the seasonal cycle to also undergo long-term changes in addition to the long-term thinning.

Due to the turn around of the moorings and the data processing, a lag in data availability is expected. However, the most recent data are not available to MOSJ yet.

2.1.7 Barents Sea/Hopen & North of Svalbard

Regular monitoring of sea ice thickness in the Barents Sea takes place only on fast ice at Hopen. Observation going back to 1966 were published by Gerland et al. (2008) and included in a previous MOSJ report (Hansen, 2010). While measurements have continued, more recent data are not available yet.

Over drift ice in the Barents Sea and in the region north of Svalbard, various campaigns have measured sea ice thickness in different years. Renner et al. (2013) compiled airborne measurements going from the ice edge north of Svalbard up to 85°N covering spring and summer. They found large seasonal changes, but little interannual variability between 2007-2011, suggesting that the area is almost entirely dominated by first and second-year ice, the thickness of which is dominated by thermodynamic processes. During the N-ICE2015 campaign, a 5-month drift expedition in spring 2015 in the pack ice in roughly the same region north of Svalbard (Granskog et al. 2016), slightly lower ice thicknesses were recorded (A. Rösel, NPI, pers. comm.). King et al. (2017) compared available sea ice thickness observations in the Barents Sea. These are restricted to upward looking sonar measurements in 1994-1996 and airborne campaigns in 2003 and 2014. They find large variability between the years depending on the dominant thermodynamic and dynamic processes, i.e. local formation versus long-range advection. While the sea ice cover in the Barents Sea is generally too thin for CryoSat-2 measurements, recent developments in thin ice thickness retrievals from SMOS and comparison to airborne thickness measurements are promising and could provide a means for future monitoring (Kaleschke et al. 2016).

2.1.8 Svalbard fjords: Kongsfjorden and Storfjorden

Regular monitoring of fjord fast ice thickness is conducted by NPI in Kongsfjorden and in Inglefieldbukta (Storfjorden). The Kongsfjorden time series was included in Hansen (2010). Preliminary results from recent years of observations at Kongsfjorden show thinner ice and snow than levels from the beginning of the recordings (Gerland and Renner 2007), but overlayed by interannual variability (S. Gerland, pers. comm.). Recent observations from Inglefieldbukta are currently summarised with the aim to publish a time series for that site.

2.1.9 Conclusions

The sea ice cover in the MOSJ region is characterised by large variability, but trends are clear. Sea ice extent in the Barents Sea and in the Greenland Sea are declining. Especially in winter, this decline of up to 12% per decade is faster than the Arctic-wide decrease. In Svalbard fjords and the region near the Svalbard coast, sea ice area and fast ice extent vary a lot from year to year, but existing time series indicate a decline and a shift towards less ice here as well. In addition to the ice retreat, the ice cover is also thinning. In Fram Strait, loss of multiyear ice and thinning of first-year ice led to a reduction in thickness of over 50% for 2003-2012. Long time series from Hopen confirm thinning of fast ice over the last five decades, but time series for larger areas in the Barents Sea are missing. Occasional surveys suggest a thinning. Fast ice in Svalbard fjords is continuing to decline in thickness as well, but observations cover only few locations around Svalbard. The observed changes are mostly driven by large-scale patterns in atmospheric circulation and increased oceanic heat transport. On regional scales around Svalbard, local drivers are likely to have a significant effect, and require detailed assessment.

2.1.10 Suggestions to MOSJ

Current MOSJ indicators are capturing the state of the sea ice cover in Fram Strait and in the Barents Sea, however, Svalbard fjord ice is not included. There is ongoing monitoring activity on both the western and eastern side of Svalbard (Kongsfjorden and Storfjorden, respectively), which could easily be intergrated as MOSJ indicators. Further, Rijpfjorden on the northern coast of Nordaustlandet would be a useful site which has seen a substantial amount of research effort from various actors (e.g. NPI, UNIS) and which would complement the other two potential fjord locations. Since the fjord ice cover is much more intimately linked to local processes than the ice cover in the Greenland Sea or the Barents Sea, regular monitoring would hugely improve MOSJ's ability to follow the development of the Svalbard marine environment.

Thanks to the recent improvements in satellite resolution and capabilities close to land, fjord ice extent and area indicators could be based on satellite data.

The current definition of the Fram Strait sea ice extent indicator covers a very large area, which goes beyond what usually is considered to be part of Fram Strait. We therefore suggest to rename the indicator to "Greenland Sea sea ice extent", as we did in this report.

2.2 Temperature and Salinity of the West Spitsbergen Current

2.2.1 The West Spitsbergen Current

The West Spitsbergen Current (WSC) is the northernmost extension of the North Atlantic Current system, which transports warm and saline subtropical waters northward across the North Atlantic and along the eastern rim of the Nordic Seas to Fram Strait. The WSC is the principal conduit through which warm Atlantic water is transported in to the Arctic Ocean. Atlantic water passing though the shallow Barents Sea loses its significant heat to the atmosphere and enters the Arctic Ocean at a temperature close to 0 °C (Schauer et al. 2003).

South of Fram Strait, the WSC has a surface temperature maximum and rapidly loses heat to the atmosphere and to sea ice drifting out of the Barents Sea. Initial interaction with sea ice rapidly cools the WSC, but the fresh meltwater released quickly forms a strongly stratified surface layer, which protects the WSC from further interaction and heat loss to either sea ice or the atmosphere. The surface meltwater layer allows the WSC to deliver heat deeper into the Arctic Ocean than would otherwise be possible. Boyd and D'Asaro (1994) find that the WSC loses heat resulting in a core cooling rate of 0.5 °C per 100 km between 74° 30' N and 81° N. When the WSC encounters denser ice in the vicinity of Fram Strait, ice melt starts to account for a larger proportion of total heat loss but the total cooling rate drops to around 0.25 °C per 100 km between 79° N and 82° N (Cokelet et al. 2008). The WSC does not only lose heat though the surface. The density gradient is very shallow below 50 m in Eastern Fram Strait and the WSC loses similar amounts of heat though mixing with adjacent water masses as it does though surface cooling (Saloranta and Svendsen 2001).

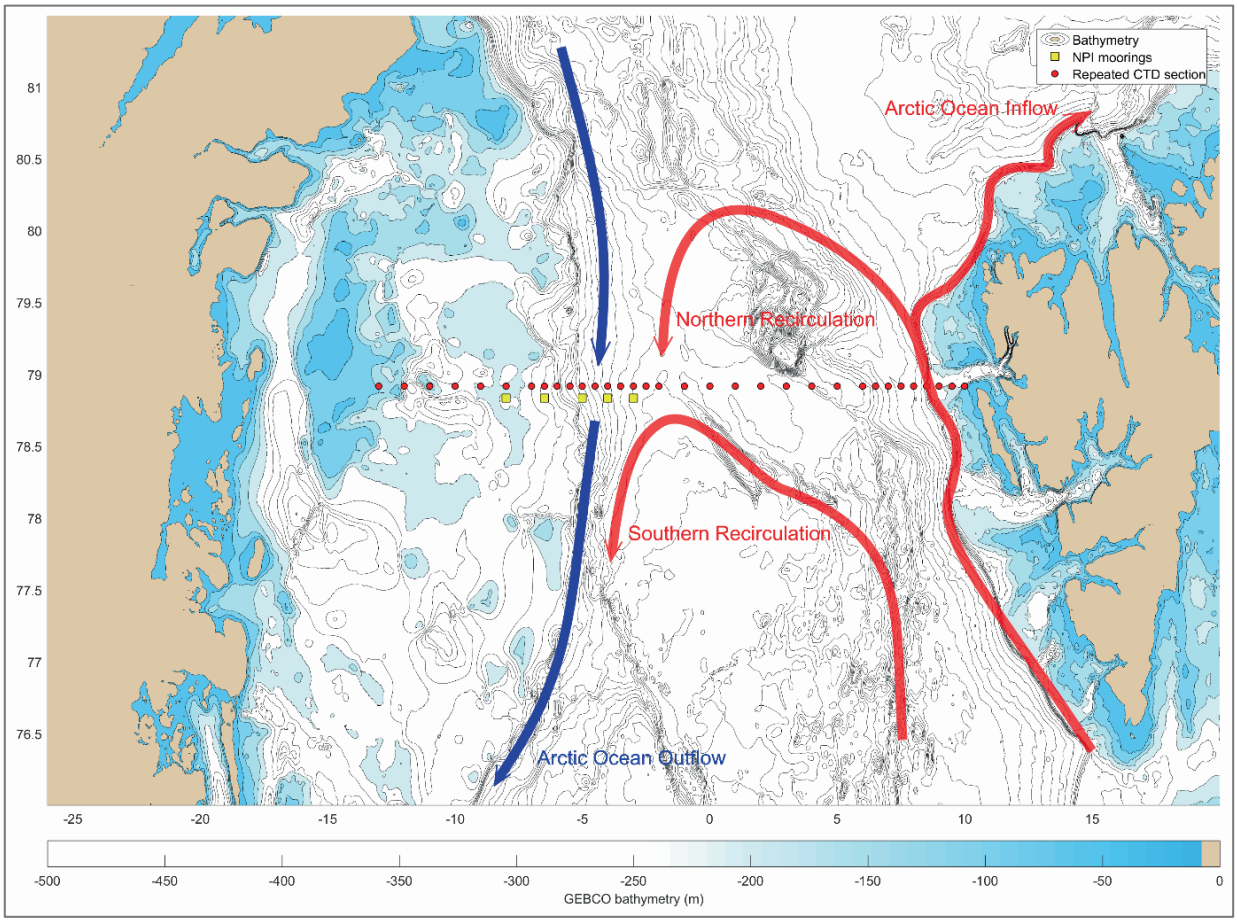

***Figure 6**: Branches of the West Spitsbergen Current (red arrows) and the Arctic Ocean outflow (blue arrow) in Fram Strait. The Norwegian Polar Institute's monitoring system (established in 1997) consists of an annually repeated hydrographic section (red circles) and moored array (yellow squares).*

The WSC is largely barotropic (Bourke et al. 1988) and predominantly follows bathymetric contours. The complex bathymetry in Fram Strait causes the WSC to split in three branches (Figure 6):

1. An Arctic Ocean Inflow Branch, which follows the top of the continental slope north and east of Svalbard, entering the Arctic Ocean and travelling around the Polar Basin before returning as part of the East Greenland Current after much modification (Aagaard, 1987).

2. A Southern Recirculating Branch, which follows the foot of the continental slope and recirculates in the vicinity of 79° N and flows south as part of the East Greenland Current (Hattermann et al. 2016).

3. A Northern Recirculating Branch, which follows topography around the Molloy Hole and re-circulates around 81° N before flowing south as part of the East Greenland Current (Hattermann et al. 2016); A mooring array jointly maintained by the Norwegian Polar Institute and Alfred Wegner Institute since 1997 records the northern recirculating branch, however there are limited observations of the southern recirculating branch.

Marnela et al. (2013) estimate that about 50% of Atlantic Water flowing northward in the WSC recirculates before passing 81° N.

2.2.2 Relevance to MOSJ

Monitoring the temperature and salinity of the WSC is important for understanding the changing climate in the Arctic (eg: Aagaard et al. 1987), changing circulation pathways in the Arctic Ocean (Rudels et al. 2015) and the local climate around Svalbard (Walczowski and Piechura 2011).

Heat supplied by the WSC makes Eastern Fram Strait the northernmost perennially ice free sea area in the world (Haugan 1999). Piechura and Walczowski (2006) find a strong correlation between the mean summer temperature of the WSC and the ice free area around Svalbard the following winter. The correlation with summer ice free areas is weaker, as solar radiation, wind stress and atmospheric heating also affect the sea ice extent in summer, while in winter oceanic heat input is the only significant factor. There is a higher correlation between local ice cover and the temperature of the northern recirculating branch of the WSC as this branch passes over the shallow Yermak Plateau where warm water has the greatest chance of interacting with sea ice. The Arctic Ocean branch subducts below a polar surface water layer and releases most of its heat further into the Arctic Ocean (Cokelet et al. 2008). Many factors contribute to the warming of the Arctic Ocean. One significant factor is the reduction of sea ice extent due to oceanic heat input, which exposes large and dark open water areas where the ocean can absorb more solar radiation and warm further (Overland et al. 2016), a process which is strongly driven by heat supplied by the WSC.

The temperature of Atlantic Water in the WSC is also the dominant factor controlling air temperature over Svalbard (eg: Beuchel et al. 2006). Walczowski and Piechura (2011) find that variations in the temperature of the WSC explain 92% of the variability in annual mean air temperatures measured at the Hornsund Station. WSC temperature is also an indicator for the ocean climate in the coastal areas of West Spitsbergen (Hop et al. 2006). Several studies have shown that the WSC temperature, or related indices can be linked to changes in the coastal ecosystems of Spitsbergen (e.g. Berge et al. 2005; Beuchel et al. 2006; Carroll et al. 2011; Hindell et al. 2012; Kwasniewski et al. 2012). The WSC also transports meroplankton (planktonic larvae of invertebrates) and fish larvae from the south, which might change the local ecosystems via an increased inflow of sub-arctic and boreal species (e.g. Berge et al. 2005).

2.2.3 Monitoring method

The temperature and salinity of the WSC are monitored using repeated hydrographic profiles penetrating the narrow core. Strong zonal temperature and salinity gradients at the edges of the current mean profiles that do not penetrate the core tend to under-estimate both temperature and salinity. As the WSC follows bathymetric contours along the shelf break, profiles within 0.25° longitude of the shelf break (as defined by the 500 m isobath) usually penetrate the core. Profiles more than 0.25° from the shelf break do not sample the core of the WSC and are not considered in this indicator.

The latitude of profiles is less critical than the longitude. However, the WSC loses heat to the atmosphere resulting in downstream cooling of approximately 0.25°C per 100 km in the region of Fram Strait (Cokelet et al. 2008). This indicator is calculated using hydrographic profiles from the narrowest

range that allows a good temporal coverage: a 44 km wide band between 78° 48’ N and 79° 12’ N. As hydrographic sections are concentrated around 79° N, the band would need to be greatly extended either to the north or south to include significantly more profiles.

The WSC has a strong seasonal temperate cycle, with maxima in August/September. Peak–to–trough temperature variations of 1.6 °C occur at the surface above the core and account for > 50% of total variance in that location. The amplitude of the seasonal cycle decreases with depth, falling to 0.5 °C (peak–to–trough) by 200 m where it accounts for <30% of total variance. (Beszczynska-Möller et al. 2012). It is critical that measurements from different seasons are evaluated separately. The majority of modern conductivity–temperature–depth (CTD) surveys in Fram Strait is carried out in August or September, but a significant minority is collected earlier in the year.

This indicator considers profiles collected between 15 August and 30 September (the 6-week period which contains the largest number of hydrographic profiles though the WSC core) from 78° 48’ N to 79° 12’ N and within 0.25° longitude of the shelf break. In years when several qualifying profiles are available, the profile closest to the 500 m isobath is selected. Where multiple profiles were collected at the same distance from the 500 m isobath in the same year, the profile collected closest to 1st September is selected.

2.2.4 Evaluation of the monitoring method

The first hydrographic survey in Eastern Fram strait was conducted in 1910, but the first profile that qualifies to be included in the indicator was collected in 1926. Although there were a number of hydrographic surveys in the intervening years, the second qualifying profile was not collected until 1962. Further qualifying profiles have been collected fairly regularly since, excepting a 9-year gap from 1964 until 1973. Since 1997, qualifying profiles have been collected annually as part of the Norwegian Polar Institute’s Arctic Ocean Outflow Observatory in Fram Strait (Figure 1). The first 47 years of the time series are somewhat less illuminating than the more recent part as inter-annual variability is not resolved.

2.2.5 Results

General Hydrographic Situation

Hydrographic profiles collected in 35 different years between 1926 and 2016 qualify for inclusion in the indicator (locations shown on Figure 7). The qualifying profiles reveal the WSC in Fram Strait to have a subsurface salinity maximum of 35.0 to 35.1, which occurs between 25 and 50 m (Figure 8, top panel). The salinity maximum is generally isolated from the surface by a fresh (salinity less than 34.7) layer, as it is further south (eg: Beszczynska-Möller et al. 2012). Below the surface layer, the WSC is not strongly stratified in salinity, although a weak halocline generally occurs around 200 m and separates the most saline part of the WSC from deeper, fresher waters. The salinity core of the WSC can therefore be described as occupying the depth range from 25 to 200 m in Fram Strait.

In most years the WSC exhibits a subsurface temperature maximum, which occurs just above the salinity maximum (Figure 8, upper middle panel), but in some years the temperature maximum occurs right at the surface, within the fresh surface layer. This variability makes it difficult to define an upper boundary

for the temperature core of the WSC. A lower boundary is more easily defined as a thermocline generally coincides with a weak halocline around the 200 m and separates the warm core from slightly cooler waters below.

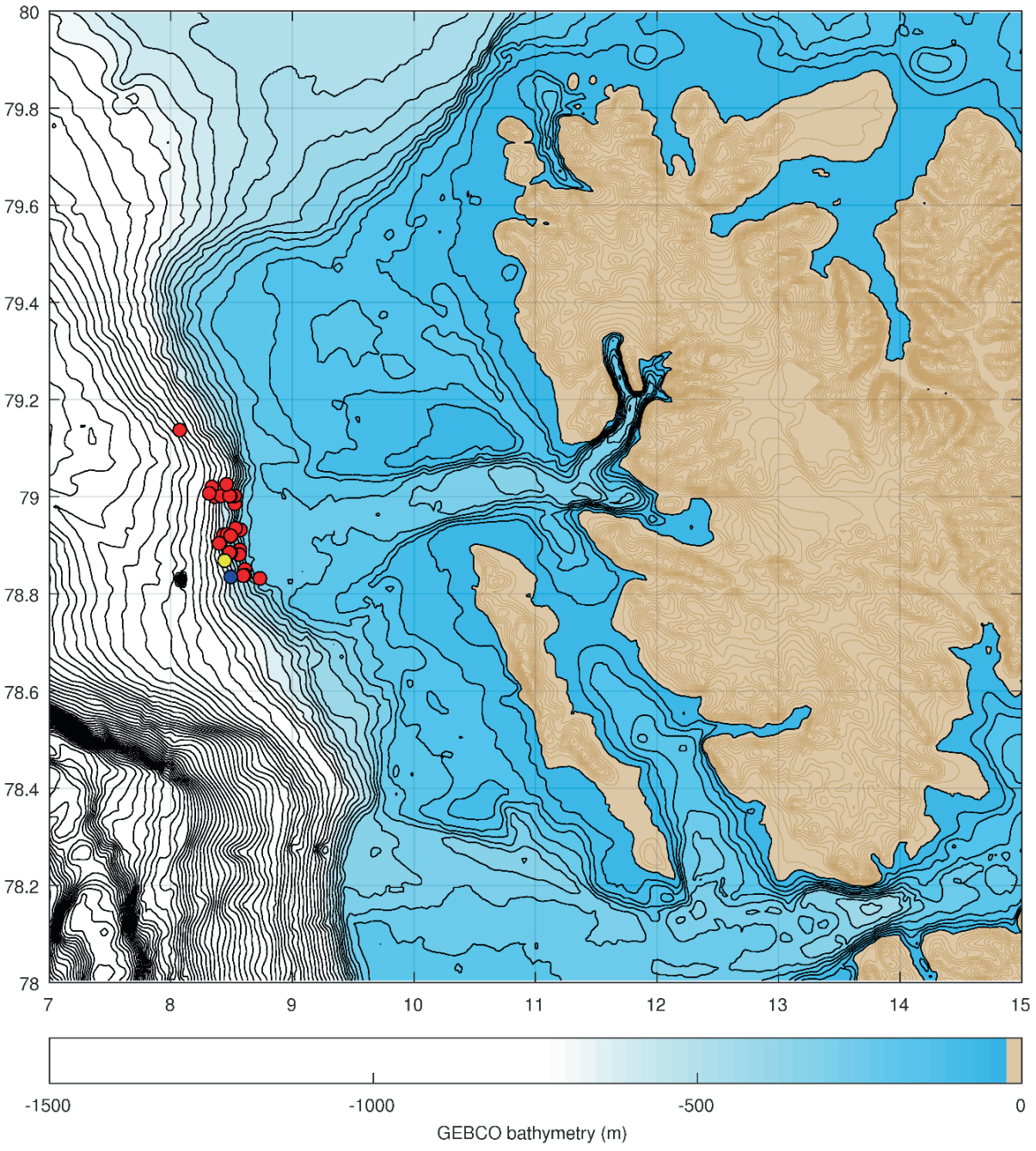

***Figure 7**: Locations of late summer (August 15 – September 30) hydrographic profiles collected from the core of the West Spitsbergen Current between 1926 and 2016. The warmest (and most saline) profile from 2006 is highlighted in yellow and the coolest (and freshest) profile from 1998 is highlighted in blue. Bathymetric contours are drawn at 50 m intervals.*

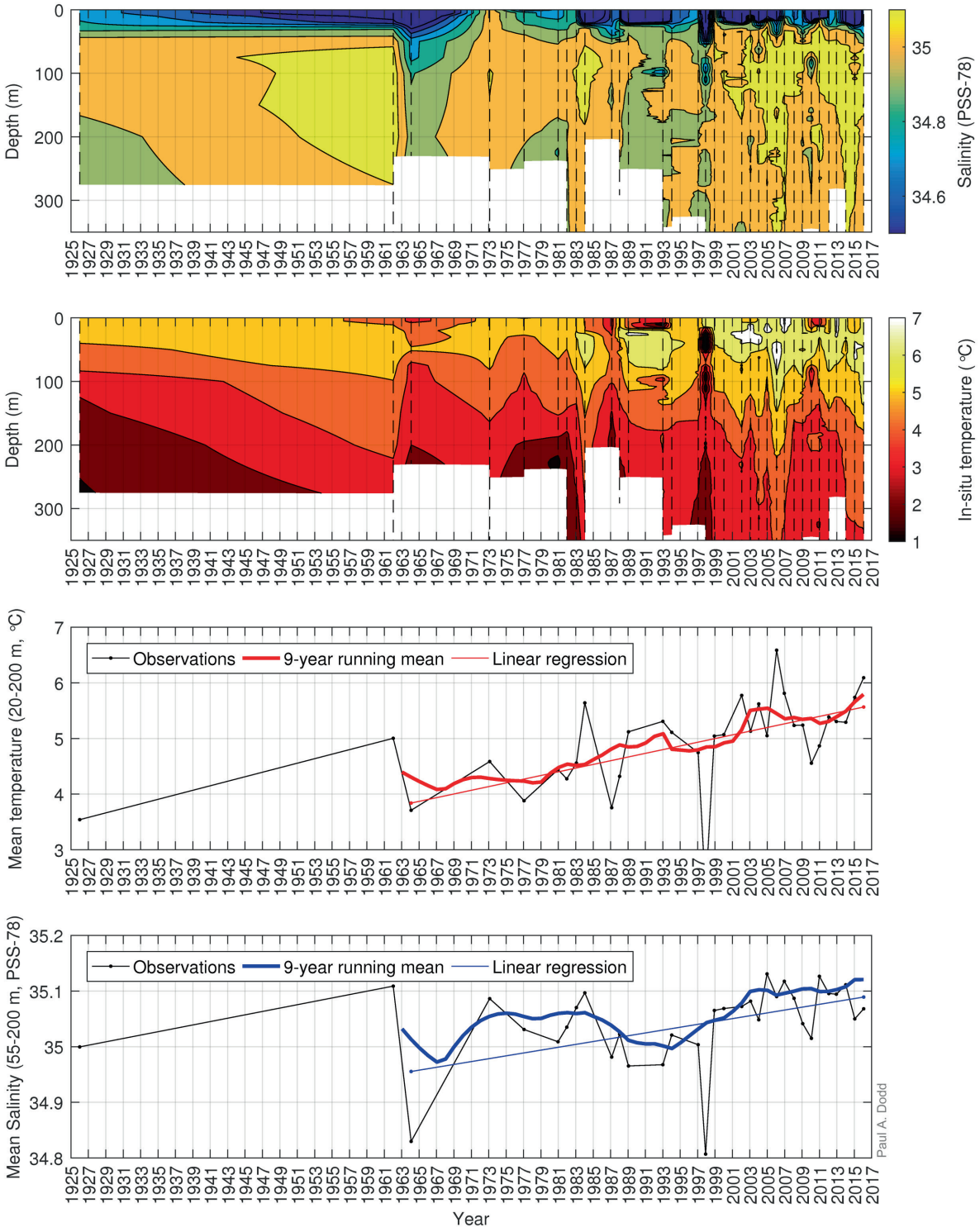

***Figure 8**: Upper panels: Hovmöller diagrams showing the evolution of salinity and temperature in the core of the West Spitsbergen Current between 1926 and 2016. Dashed vertical lines indicate times when profiles were collected. Lower panels: evolution of mean temperature and salinity in the core of the WSC at times when CTD profiles were collected; Linear regression of values at times when profiles were collected (fine, coloured lines); 9-year running means (bold, coloured lines). Values for years without observations were first estimated by linear interpolation before running means of the interpolated time series were calculated.*

Temperature Changes

The 9-year running mean of (annually interpolated) mean temperatures between 20 and 200 m in the core of the WSC (Figure 8, lower middle panel, bold red line) increased from 4.4 °C in 1963 to 5.8 °C in 2016; an increase of 1.4 °C in 52 years, or 0.27 °C per decade. A linear regression of the mean temperatures between 20 and 200 m at times when profiles were collected (Figure 8, lower middle panel, fine red line) shows an increase from 3.8 °C in 1963 to 5.6 °C in 2006; an increase of 1.7 °C in 52 years or 0.33 °C per decade. Both approaches predict comparable long-term warming rates. No trend is estimated for the period before 1963 as the sparse observations collected before 1963 do not resolve the inter-annual variability that is seen in the later part of the time series.

While there is a clear warming trend, a number of temperature anomalies also occur in the time series. The most pronounced occurred in 2006, when the highest mean core temperature was observed (6.6 °C, Figure 8, lower middle panel, black line). Temperatures remained high from 2002-2007 so that the 2006 maximum can be considered part of a 5-year anomalously warm period. The 2006 warm anomaly was not limited to the core depth range, but affected the whole water column, depressing the 4 °C isotherm by more than 150 m relative to the pre (1988-2000) and post (2008-2013) mean depths (Figure 8, upper middle panel).

Another warm anomaly occurred in 1984. There is no evidence of a warm period surrounding the 1984 anomaly as there was around the 2006 anomaly (Figure 8, lower middle panel, black line), but this may be partly due to a lack of observations in 1985 and 1986. Curiously both the 1984 and 2006 warm anomalies were followed by pronounced local temperature minima 3-4 years later, but with only two cases, this cannot be considered a significant pattern.

Current (2015, 2016), core temperatures are very high and the 4 °C isotherm is currently displaced downwards more than 100 m relative to the 2008-2013 mean depth, as it was during the 2002-2007 warm period surrounding the 2006 warm anomaly.

The temperature profile collected in 1998 (Figure 8, upper middle panel) is anomalously cool and produces a low spike in the time series (Figure 8, lower middle panel). The 1998 profile shows extensive interleaving with a cooler, fresher watermass in the core of the WSC, which is probably not uncommon as there is little density gradient to prevent it. Similar, but less extensive inter-leaving can be seen in the 1987, 1993, 2004 and 2008 profiles. The interleaving seen in the 1998 and other profiles, facilitates the isopyncal mixing though which the WSC loses around half of its heat content (Saloranta and Svendsen 2001).

Temperatures within the fresh surface layer are highly variable and do not co-vary with temperatures in the 20 – 200 m core. Moreover, there is no strong relationship between temperature and salinity in the fresh surface layer. If the surface layer was mostly produced by local sea ice melting as a result of ocean heat supplied by the WSC a stronger correlation would be expected. The lack of correlation suggests that either solar radiation and atmospheric heating play a large role in late summer, as proposed by Piechura and Walczowski, (2006), or that the surface layer is significantly influenced by water from the continental shelf, or Sørkapp current.

Salinity Changes

Below the fresh surface layer temperature and salinity in the WSC co-vary (c.f. Figure 8 lower middle and bottom panels, black lines). Local temperature maxima (1984, 1994, 2006) have high salinities, while local temperature minima (1964, 1987, 2010) have low salinities. However, the relationship is not perfectly synchronised and local temperature and salinity minima are often separated by +/- 1 year.

The mean core salinity varies more smoothly than the mean core temperature, while there was an extreme peak in core temperature in 2006, the core salinity in 2006 was highly elevated for a 3- year period around the temperature peak (2005-2007). The same pattern occurred before the 1984 temperature peak; in both cases elevated salinities were observed in the year before the temperature peak occurred.

The 9-year running mean of (annually interpolated) mean salinity between 55 and 200 m in the core of the WSC (Figure 8, bottom panel, bold blue line) increased from 35.02 in 1963 to 35.12 in 2016; an increase of 0.1 in 52 years, or 0.02 per decade. A linear regression of the mean salinity between 55 and 200 m at times when profiles were collected (Figure 8, bottom, fine blue line) shows an comparable increase from 34.96 in 1963 to 35.09 in 2016; 0.13 °C in 52 years or 0.026 per decade. Though the 9-year running mean is rather strongly affected by very high salinities measured in 1962.

Comparing the mean core temperature and salinity of the WSC in each year that observations are available (Figure 9) reveals that warmer profiles are not sufficiently more saline so as to maintain a constant density. The present, warmer WSC is therefore also less dense; in 2006 the core was more than 0.2 kg m^{-3} less dense than it was at some times during the late 1970s and early 1980s.

A very saline profile measured in 1962 plots just at the edge of the main envelope of profiles in temperature – salinity space, but in a feasible position with respect to density. A subsequent 1964 profile is anomalously fresh and plots some way outside the main envelope, but also in a feasible position with respect to density. Due to sparse sampling these two anomalous profile dominate the early part of the time series but their position in temperature – salinity space gives no new insight into their validity.

In addition to the 1962 and 1964 profiles, two profiles from 1989 and 1993 also have a notable position in temperature – salinity space. The 1989 and 1993 profiles are some of the least dense recorded, but are not especially warm. The low density is due to a low salinity anomaly, which affected the full depth of the water column below the fresh surface layer (Figure 8, upper panel). These profiles seem to have been influenced by the Great Salinity Anomaly of the 1980s (Belkin et al. 1998), which crossed the Sørkapp section south of Svalbard in 1988 and would have reached Fram Strait in 1989 (Belkin et al. 1998, their Figure 2). These 1989 and 1993 profiles may constitute the furthest downstream observation of the 1980's Great Salinity Anomaly.

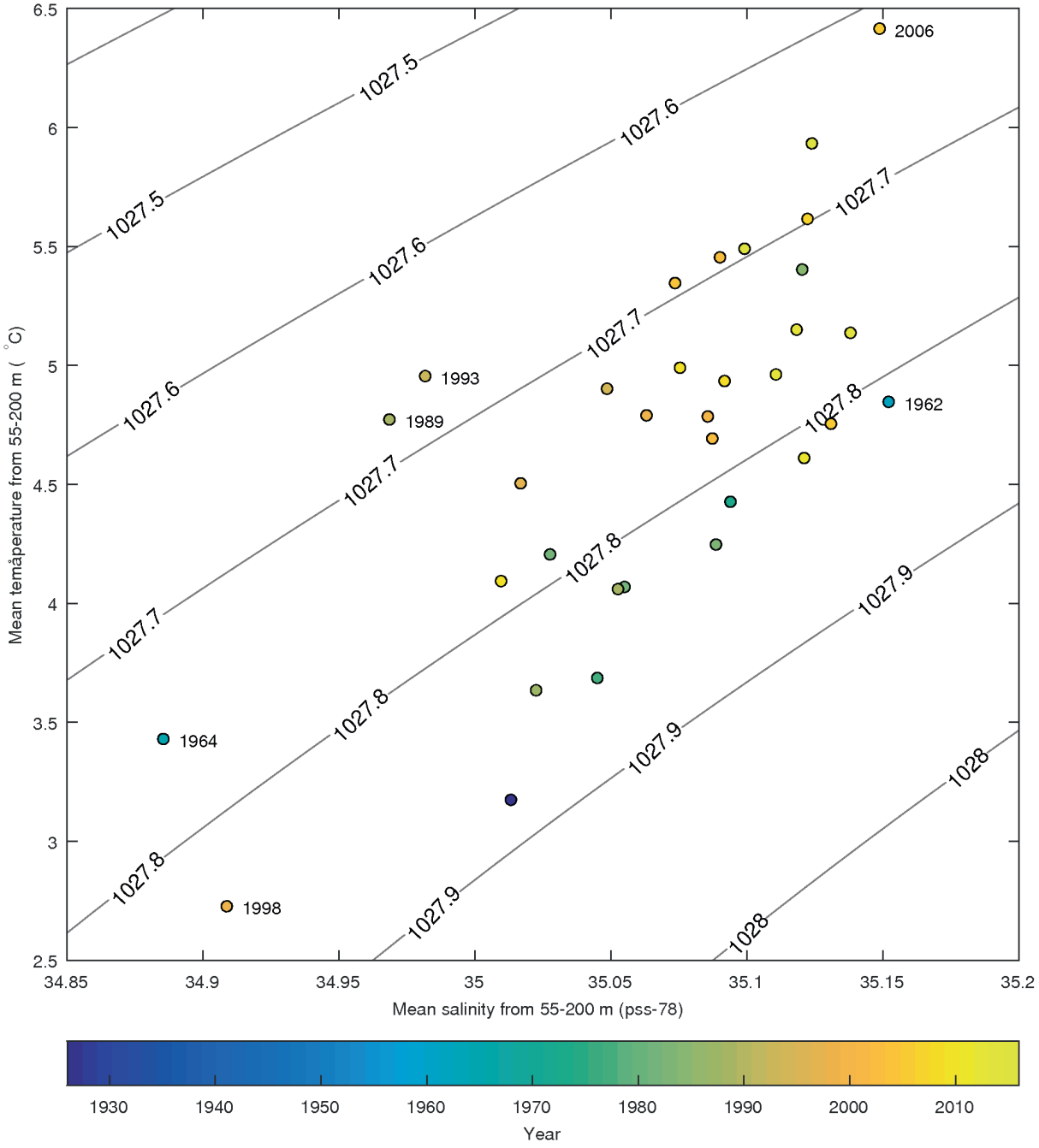

***Figure 9**: Temperature-salinity diagram showing the evolution of mean hydrographic properties in the core of the West Spitsbergen Current between 1926 and 2016. Dates of anomalous profiles are indicated next to points. Contour lines indicate density in kgm^{-3}. Variations in mean salinity explain 71% of the variance in mean temperature, the correlation is significant at the 99% level.*

2.2.6 Discussion and Conclusions

The warming trend detected in the WSC is consistent with observations collected by an array of hydrographic moorings deployed across Fram Strait from 1997 to present (Beszczynska-Möller et al. 2012), but the rates of warming determined by the two approaches are very different: 0.3 °C per decade (this study) and 0.6 °C per decade (Beszczynska-Möller et al. 2012). However, it is inappropriate to make *quantitative* comparisons, as the results are highly dependent on the region and depth range used. Moreover, this indicator captures only the late summer situation while Beszczynska-Möller et al. (2012) describe annual mean temperatures. However, both studies detect the most pronounced anomalies in the time series: the warm/saline anomaly of 2005-2007 and the cold/fresh anomaly of 1998.

Both the long term warming trend and local temperature anomalies observed in the WSC can been linked to changes in the sub polar north Atlantic. Polyakov et al. (2008) find that the upper 2000 m of the North Atlantic warmed by 0.03 °C per decade from 1920 to 2000. Polyakov et al.'s rate of warming is only 1/10th of the rate estimated between 20 and 200 m in the WSC, but is averaged over the top 2000 m. Much of the warming that Polyakov et al. (2008) report is likely to have occurred in the upper layers and the mean temperate change within those upper layers was likely much larger.

Hátún et al. (2005) identify upper ocean temperature and salinity maxima in the sub-polar North Atlantic in 1997-98 and 2003. Assuming a 2-3 year lag (eg: Polykov et al. 2005) the 2003 anomaly corresponds with the 2006 anomaly observed in Fram Strait. This study did not detect a warm anomaly in the WSC corresponding with the 1997-8 anomaly in the sub-polar gyre, but Beszczynska-Möller et al. (2012) observed a warm anomaly in western Fram Strait in 2000 which was presumably conveyed via the WSC.

The sparse observational record in Fram Strait is too short to fully investigate the causes of inter-decal (or longer term) variability in the properties of the WSC, and that question is beyond the scope of this work. However, as the warming signal seems to have been advected from downstream we briefly discuss the dominant modes of variability in the North Atlantic, which have the potential to affect the WSC.

As the WSC is an extension of the North Atlantic Current, it has been suggested that properties might correlate with the North Atlantic Oscillation (NAO) index (eg: Polyakov et al. 2008), which entered a positive phase in the mid 1990s after a long negative phase beginning in the early 1960s. During positive phases of the NAO there is an enhanced circulation in the entire meridional overturning circulation, including the northward transport of warm subtropical Atlantic water in the north Atlantic Current. Holiday et al. (2008) proposed the positive NAO-state as a factor contributing to warming of the Norwegian Atlantic Current from 1995 to present, but it is probably not the only factor. Air temperature over the Nordic Seas, which modulates cooling to the atmosphere (eg: Furevik et al. 2001) and the rate of advection (eg: Karcher et al. 2003) have also been proposed as significant influences.

The Atlantic Multi-Decadal Oscillation (AMO) (e.g.: Kerr 2000) describes the North Atlantic sea surface temperature (SST) relative to the global mean SST. The AMO has been related to heat transport in the Atlantic Meridional Overturning Circulation (AMOC), of which the WSC is an extension, such that the North Atlantic SST warms when the AMOC speeds up (Delworth & Mann 2000). The AMO has a period of 60-80 years (Delworth & Mann 2000) and was positive from 1950 until the late 1960s after which it entered a negative phase which lasted until the late 1990s. In recent years the AMO has again been

positive (NOAA, 2017). The warming trend observed between 1962 and 2016 in Fram Strait may therefore be enhanced by the AMO which moved from a negative phase at the beginning of the observational period into a positive phase at the end. It is unclear to what extent the AMOC directly drives the AMO and to what extent the atmospheric circulation is responsible, however using model simulations O'Reilly et al. (2016) showed that the AMO is at least not driven by mid-latitude atmospheric forcing. Recent work by Zhang (2017) also supports the idea that oceanic forcing plays a dominant role in forcing the AMO.

On short time scales, the core temperature of the WSC in Fram Strait is likely to be a good predictor of the local climate and sea ice extent around Svalbard, as local direct heat loss to the atmosphere and strong tidal mixing over shallow bathymetry release heat from the WSC. Further into the Arctic Ocean, Atlantic Water is separated from the surface by a fresh surface layer, which inhibits vertical heat transport. Further into the Arctic Ocean, variability in the energy available for vertical mixing derived from sources such as wind forcing and flow over bathymetry, which is needed to release heat from the Atlantic layer, may be at least as important as the temperature of water within the Atlantic layer in predicting the state of Arctic sea ice.

The majority of observations for this indicator are provided by the long term Arctic Ocean Outflow Observatory in Fram Strait (Norwegian Polar Institute, 2017), which is one part of an Arctic-wide monitoring system that collects long-term observations across all the major Arctic Gateways. Maintaining an effective Arctic-wide monitoring system is an important task for the international Arctic research community.

2.2.7 Suggestions to MOSJ

While the early part of the time series provides a kind of baseline, annual measurements are needed to capture the high frequency variability observed in recent years. It is important that the 1997-2016 annual sampling programme is maintained. The indicator only describes the late summer situation as there are insufficient observations to build a time series at any other time of year. Augmenting the monitoring program to provide winter observations would be worthwhile, as winter is the season when the link between local sea ice extent and ocean heat input is strongest (Piechura and Walczowski 2006) and late summer observations of the WSC may not accurately describe the winter situation, when different processes may dominate.

Collecting CTD measurements from the West Spitsbergen Current during the Norwegian Polar Institute's 2016 Fram Strait cruise. The Fram Strait CTD section has been repeated annually since 1997 as part of the Fram Strait Arctic Outflow Observatory. Photos: Paul A. Dodd, Norwegian Polar Institute.

2.3 Hydrography and freshwater in Svalbard fjords: Kongsfjorden, Tempelfjorden and Rijpfjorden

There is currently no indicator developed for monitoring the hydrography in Svalbard fjords. However, water properties are important for the assessment of e.g. ocean acidification; we therefore include a short summary of the main features here.

The fjords in west-Spitsbergen and north of Svalbard (Kongsfjorden, Rijpfjorden) are highly stratified due to several water layers of fresh surface layer in summer (SW), intermediate water (IW), transformed Atlantic water (TAW) in the middle to outer part, and local fjord water (LW) in the deeper part of the fjord, including winter cooled water (WCW) mainly in the inner parts of the fjords (Hop et al. 2006). The TAW is dominated by Atlantic water (AW), which has its origin in the West-Spitsbergen Current (WSC) and is mixed with Arctic water (ArW) on the shelf when it is advected into the fjords (e.g. Kongsfjorden, Tempelfjorden; Cottier et al. 2005). The fjords are largely affected by meltwater discharge from glaciers, particularly near the glacier fronts but also within and outside the fjords (Keck et al. 1999; Hop et al. 2002, 2006; Svendsen et al. 2002), which results in strong surface stratification during summer. As an

effect of increased WSC, the fjord water is expected to become warmer resulting in larger discharge of meltwater into Kongsfjorden (Piquet et al. 2014).

2.4 Ocean acidification

2.4.1 Introduction: Ocean acidification and definition of saturation and effect on pteropods

Calcium carbonate ($CaCO_3$) saturation (Ω) is used as a chemical indicator for the dissolution potential for solid $CaCO_3$ and for ocean acidification (OA) state. When $\Omega < 1$, solid $CaCO_3$ is chemically unstable and prone to dissolution (i.e., the waters are undersaturated with respect to the $CaCO_3$ mineral). $CaCO_3$ occurs in several solid forms including aragonite (a) and calcite (c) where aragonite is less stable than calcite. Marine biogenic $CaCO_3$, such as shells and skeletons of marine organisms, is biologically formed using a variety of mechanisms involving bicarbonate (HCO_3^-), carbonate ion (CO_3^{2-}) and CO_2 (Findlay et al., 2011). The dissolution of $CaCO_3$ is controlled by the concentrations of CO_3^{2-} and calcium (Ca^{2+}) in the water, and depends on salinity, temperature and pressure (Ingle 1975; Mucci 1983). In ocean acidification field studies, Ω is thus an indicator for a chemical change in the $CaCO_3$ dissolution potential, but is not always directly related to the biological consequences of ocean acidification. Recent studies on calcifying organisms, in particularly aragonite-forming organisms, have found clear indications for linkages between Ω_a (saturation of aragonite) and the integrity of the $CaCO_3$ structures of these organisms under future ocean acidification conditions. The free-swimming pelagic pteropod mollusc *Limacina helicina* is one of few marine organisms (taxa) that produce aragonite shells instead of calcite shells (Fabry et al. 2008; Bednaršek et al. 2012). This species has been shown to have difficulty in regulating the carbonate chemistry in their internal calcifying fluid at $\Omega < 1.4$, and consequently they are more sensitive to ocean acidification than other calcifying organisms (Ries et al. 2012; Bednaršek et al. 2014).

2.4.2 Monitoring method

Currently, there is no developed indicator for ocean acidification included in the MOSJ monitoring. Previously, observations of the carbonate chemistry and ocean acidification state (OA) in Svalbard fjords were few. During the mesocosm study in Kongsfjorden in 2008-2009 in the European Project on Ocean Acidification (EPOCA) project, data was collected (PANGEA data base). In Fram Strait (at 79° N), few ship-based observations of the carbonate chemistry (e.g. anthropogenic CO2) were performed (e.g Jeanson et al. 2008; 2010). However, time-series in the Fram Strait area (at 79° N) were lacking, particularly on the western side, in the East Greenland Current (EGC), where the physical-chemical properties of Arctic Ocean outflow water can be observed (Chierici et al. 2013). With the Fram Centre Ocean Acidification flagship and collaboration between the Norwegian Polar Institute and the Institute of Marine Research, a new field-sampling project was initiated with extensive water-sample collection and analyses of the carbonate chemistry (e.g. pH, A_T, total dissolved inorganic carbon, pCO_2, aragonite saturation) in Fram Strait (79° N) and around Svalbard. However, there are still knowledge and data gaps in inter-annual and seasonal carbonate chemistry (ocean acidification) from Svalbard fjords, in particular in winter. These gaps include the distribution and effect of ocean acidification on pteropods *Limacina helicina* in other seasons than summer (study life cycle) and in other Svalbard fjords than Kongsfjorden, Tempelfjorden,

Storfjorden and Rijpfjorden. In 2016-2017, a CO_2 sensor successfully recorded seasonal CO_2 data in Kongsfjorden.

2.4.3 Carbonate chemistry and calcium carbonate saturation variability in Svalbard fjords: Kongsfjorden, Tempelfjorden and Storfjorden

The carbonate chemistry and calcium carbonate ($CaCO_3$) saturation state in Svalbard fjords vary due to location in the fjords, between seasons and years as a result of several biogeochemical processes, such as changes in salinity and temperature, primary production, vertical mixing, ocean uptake of atmospheric CO_2, freshening, warming and sea-ice processes (Fransson et al. 2015; 2016). Increased freshwater supply in the fjords tend to decrease Ω and total alkalinity (A_T) hence increasing OA (Fig. 10; Fransson et al. 2015; 2016). Primary production on the other hand, consumes CO_2 hence increasing Ω (decrease OA). Large variability in the carbonate chemistry has been observed between years in the fjords due to differences in air temperature, sea ice conditions, and precipitation. In addition, with climate change, such as warming and increased meltwater of sea ice, ice caps and glaciers, OA is predicted to increase (AMAP, 2013).

A researcher collecting newly-formed sea ice from Tempelfjorden, Svalbard. Photo: Jago Wallenschus, Norwegian Polar Institute, 2012.

a)

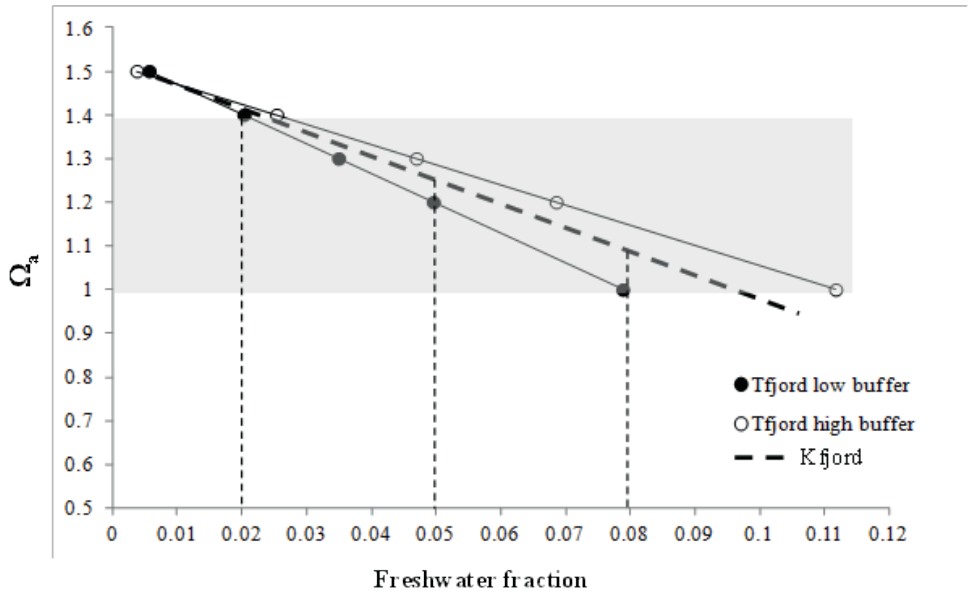

b)

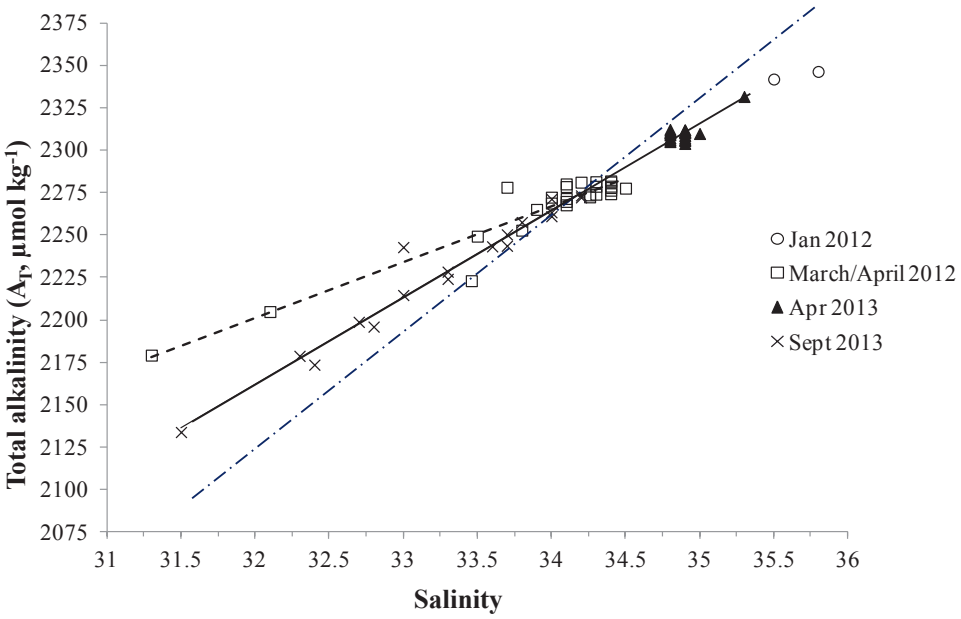

Figure 10 *a) Linear relation between aragonite saturation (Ωa) and freshwater fraction in Kongsfjorden (Kfjord) and Tempelfjorden (Tfjord; black circle is low calcium carbonate effect; open circle is high calcium; Fransson et al. 2016), and b) Linear relationship between salinity (x-axis) and total alkalinity (AT, µmol kg-1, y-axis) in Tempelfjorden during January 2012 (open circles), March and April 2012 (open squares), April 2013 (filled triangles) and September 2013 (crosses). The linear relationships were for: winter 2012 (March and April 2012) AT= 33.08x + 1142, R^2 = 0.901, dashed line; for all values in 2013 (April 2013 and Sept 2013), AT = 51.13x + 526, R^2 = 0.984, black line. The intercept of the linear relationship at zero-salinity based on 2013 values was AT =66.54, R^2 = 0.895, dashed dotted line. From Fransson et al. (2015).*

In Kongsfjorden, the aragonite saturation state (Ω_a) varies between years, season and location in the fjord (Fransson et al. 2016). In 2013, Ω_a was generally lower than in 2014 in the surface water inside the fjord. At all stations, including the shelf and slope, Ω_a decreased with depth. The lowest Ω_a (1.6) in 2013 was found in the deeper parts of the outer shelf (station V6; Fig. 11) at 250-300 m in late winter and in 2014 (1.51) in the bottom water of the outer fjord (station Kb0). In 2013, low Ω_a was also found at more shallow depths (from 25 m to below 200 m) on the shelf (Fig. 11). These Ω levels in Kongsfjorden are near or approaching the critical limits of 1.4 when the pteropod *L. helicina* has shown damage to the aragonite shell ($\Omega < 1.4$; Ries et al. 2012; Bednarsek et al. 2014). The trend and variability of calcite saturation (Ω_c) were similar to those for Ω_a but with higher values (3.5) near the glacier front in summer, increasing to $\Omega_c > 4$ (2014) in the outer parts of the fjord and on the slope (station V6).

In 2013, Ω_c decreased from the glacier front to the outer parts of the fjord (station Kb0). pH_T also varied between years, season and location and in 2013 pH_T was lower than in 2014 at the same depth and location, according to Fransson et al. (2016). In 2013, the lowest pH_T (8.06) was found on the shelf below 200 m. In 2013, the lower seawater salinity and temperature than in 2014 suggested that the Transformed Atlantic Water (TAW) was more influenced by mixing with water transported by the coastal current (CC), rich in CO_2. In addition, there was more glacial water in 2013 than in 2014. Consequently, the Ω_a and pH_T values in 2013 were lower than in 2014. The effect of glacial water in the surface water at the glacier front was prominent (10-11% freshwater fraction in both years), resulting in decreased Ω_a by 45-54%. The counteracting process of biological carbon uptake in summer increased Ω_a by the similar strength of 46-55% (Fransson et al. 2016). The direct warming effect on Ω_a showed that Ω_a increased by 0.009 per 1 °C increase and showed that temperature had a minor effect of 4% of the total Ω_a change due to combined temperature, freshening and biological carbon uptake (Fransson et al. 2016).

Researchers collecting samples from sea ice from Kongsfjorden, Svalbard. Photo: S. Gerland, Norwegian Polar Institute, 2013.

a)

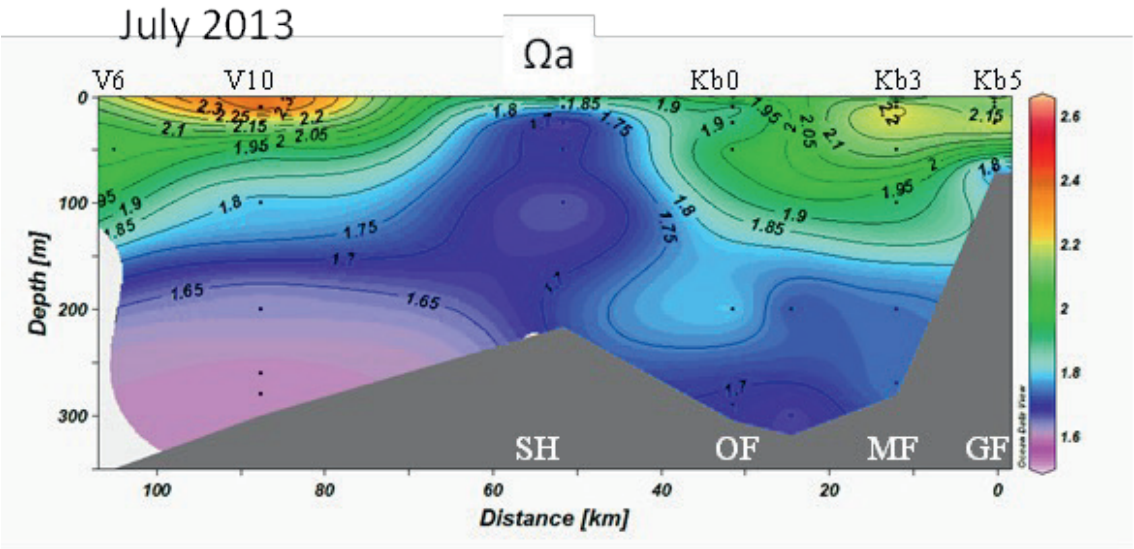

b)

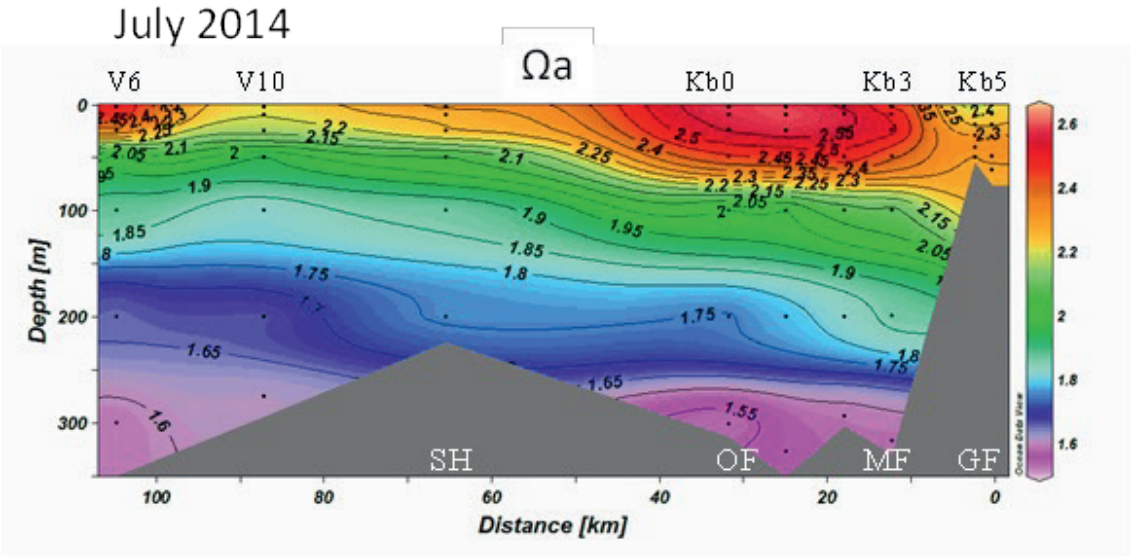

***Figure 11**. Section of aragonite saturation (Ωa) in Kongsfjorden in July a) 2013 and b) 2014. GF is glacier front, MF is mid-fjord, OF is outer fjord and SH is shelf. The stations Kb0-Kb5 are in the fjord and V6 and V10 are outside the fjord (Fransson et al. 2016).*

In Tempelfjorden in April 2012, the water under the sea ice was warmer and fresher than in April 2013 (Fransson et al. 2015). Particularly near the glacier front, there was a larger amount of freshwater in the water column under the ice than in the mid and outer parts of the fjord. Consequently, in April 2012, Ω_a and pH_T were lower near the glacier front than in April 2013, and compared to the other parts of the fjord. In total, the effect of glacial drainage water decreased Ω_a to a minimum of 1.5 increasing ocean acidification. However, although total alkalinity (A_T) was diluted by freshwater addition from the glacial

water, $CaCO_3$ particles in the glacial water originating from the bedrock, added total alkalinity (Fig. 10b). Consequently, these minerals to some extent mitigated the effect of ocean acidification as indicated by the relatively high A_T at zero salinity (i.e. glacial drainage water) as the result of addition of carbonites (Fig. 10b; Fransson et al. 2015).

In Storfjorden, the water masses are different than Kongsfjorden and Tempelfjorden with more influence by Polar Water and ice formation. There is a polynya where ice formation and deep-water formation are taking place. When sea ice is formed, dense, high-salinity brine is produced and rejected from the ice to underlying water. In the Arctic, this heavy brine also brings CO_2 from the surface water to deeper water layers (e.g. Fransson 2013). This sinking of brine with CO_2 has shown to increase CO_2 and dissolved inorganic carbon (DIC) hence decreasing Ω and pH in the bottom waters of the fjord (Anderson et al. 2004).

2.4.4 Fram Strait and variability in calcium-carbonate saturation

In the Fram Strait, on the eastern side, there is Atlantic Water (AW) inflow to the Arctic Ocean (see section 2.2) and on the western side there is Polar Water (PW) outflow from the Arctic Ocean. The different water masses and characteristics of the inflow and outflow waters affect the carbonate chemistry hence the Ω (OA state). In the western part of the Fram Strait, the Polar water in the surface brings cold and relatively low surface-water salinity water southward along the east Greenland coast in the East Greenland Current. This surface water (upper 70 m) has relatively low Ω and high CO_2 content (i.e partial pressure of CO_2, pCO_2) Data of surface-water carbonate chemistry from a period of six years shows variability, and the lowest Ω was observed in year 2012 in the upper 70 m (Chierici et al. 2015). This low Ω water (and high CO_2) was suggested to originate from the Arctic shelves. In the eastern part of Fram Strait, AW brings warm and high-salinity water, rich in CO_2 and nutrients, into the Arctic Ocean. This warm water also contributes to the melting of sea ice and glacial ice (e.g in Kongsfjorden), consequently lowering Ω.

2.4.5 Future predictions and projections; extremes

Predicted increased freshwater addition due to melting of glaciers and sea ice as the result of warming (Piquet et al. 2014) will decrease $CaCO_3$ saturation and increase ocean acidification. Winter-surface and bottom water Ω may further decrease due to increased accumulated freshwater from summer melt, which will have implications for calcifying organisms.

Previous studies show that the AW contains high amounts of anthropogenic CO_2 (e.g. Sabine et al. 2004), due to efficient anthropogenic CO_2 uptake during cooling as the AW is transported northward along the Norwegian Coast. Olsen et al. (2006) estimated the rate of fCO_2 increase due to anthropogenic CO_2 uptake to be about 1 µatm yr^{-1} in the WSC and on the West Spitsbergen shelf, which will increase ocean acidification. A model study by Skogen et al. (2014) predicted a doubling of the ocean CO_2 uptake (2000-2065) from 23 to 37 $gCm^{-2}yr^{-1}$ in the WSC and AW, resulting in a decrease of pH by -0.19 in this period. Fransson et al. (2016) assumed two scenarios in Svalbard fjords: 1) colder and less saline (Arctic regime), and 2) warmer and more saline (Atlantic regime). For example, in Kongsfjorden the Transformed Atlantic Water (TAW) is influenced by the inflow of either a larger component of colder and less saline (and lower Ω_a) water transported by the coastal current (CC), or influenced by the inflow

of warmer and more saline AW (higher Ω_a). Freshwater supply also decreases Ω_a and increases ocean acidification, and this effect may be greater in a warmer scenario due to higher glacial water discharge. In Kongsfjorden, increased meltwater runoff from the glaciers due to enhanced warming is expected in the future (Piquet et al. 2014), resulting in decreased Ω_a. This scenario will potentially cause multi-stress impacts on calcifying organisms such as *L. helicina*, by generating physiological stress due to lower salinity, higher temperatures, and increasing the risk of dissolution and thinning of their aragonitic shells (Fransson et al. 2016).

2.4.6 Suggestions to MOSJ

Development of an indicator for monitoring carbonate chemistry and thus ocean acidification is urgently needed. To fill some seasonal and inter-annual data gaps on carbonate chemistry and ocean acidification, we recommend adding CO_2 and pH sensors, for autonomous measurements, to existing and planned moorings in Svalbard fjords, Fram Strait and north of Svalbard. In 2016-2017, a CO_2 sensor successfully recorded seasonal CO_2 data in Kongsfjorden. We also recommend continuation of already started time-series in Fram Strait and Kongsfjorden but also new time-series for long-time monitoring in other fjords. For chemical indicators of ocean acidification, we recommend calcium carbonate (e.g. aragonite saturation, Ω), pH and pCO_2. Sampling of pteropods *Limacina helicina* has taken place in Kongsfjorden and Rijpfjorden from 2013-2016 but there is a need for sampling during other seasons and in other Svalbard fjords as well. There is also a need for method development and study of the effect of OA on pteropods.

2.5 Sea level

2.5.1 Introduction

Changes in sea level are caused by various factors linked to changes in virtually all components of the climate system, making sea level rise an important indicator for MOSJ. Sea level rise varies temporally and spatially, as do the contributing processes. Major contributors are thermal and saline expansion of the ocean, atmospheric drivers (especially wind and air pressure), and melt of glaciers and ice sheets. In Norway, Svalbard and the Barents Sea region, the retreat and disappearance of the Fennoscandian and the Barents Sea ice sheets (about 15kyr BP; Patton et al. 2017) led to an ongoing uplift of land masses (so-called glacial isostatic adjustment, GIA). Together with the more recent retreat of glaciers and local changes related to groundwater storage, sediment compaction, and tectonics, the resulting, spatially non-uniform vertical land motion can counteract the effect of mean sea level rise on the coast line, and GIA has to be taken into account when interpreting tide gauge data. As the Fennoscandian and the Barent Sea ice sheets covered much of northern Europe, including Scandinavia and Finland, the Barents Sea, and Svalbard, regional sea level changes have to be assessed keeping in mind the large-scale GIA movements. Records from mainland Norway are therefore included in MOSJ and in this report.

Global mean sea level rise is accelerating which can be seen by the change of the estimated rate of increase from 1.7 mm/yr for the period 1901-2010 to 3.2 mm/yr for 1993-2010 (Church et al. 2013).

Dominant contributors were ocean thermal expansion and glacial melt, with increasing contributions from the Antarctic and the Greenland ice sheets since the early 1990s. However, both observed sea level rise and contribution from different processes show large regional differences. Jevrejeva et al. (2013) report an average rate for the Arctic in the period 1950-2008 of 2.6 mm/yr. They include tide gauge records from Canada and Alaska whereas Henry et al. (2012) limit their study to tide gauges in Norway and the Russian Arctic and consequently find a lower rate of 1.6 mm/yr. This is in line with Limkilde Svendsen et al. (2016) who include both tide gauges and satellite altimetry and report an Arctic-wide mean sea level trend of 1.5 mm/yr.

Several studies report an acceleration in sea level rise (Church et al. 2013), both regionally and globally, in particular since the early 1990s which in the case of the Norwegian coast and Svalbard is probably related to the recent warming in the Nordic Seas and the Arctic Ocean, accelerating land ice loss, and redistribution of ocean mass due to ocean circulation (Jevreleva et al. 2013; Henry et al. 2012). Simpson et al. 2015, find a similar acceleration using Norwegian tide gauges only. Richter et al. (2012) find a strong contribution of the so-called inverse barometer effect, where atmospheric pressure influences sea level, to temporal sea level variability along the Norwegian coast. Nevertheless, thermal expansion of the ocean is the largest contributor to the linear trend. Calafat et al. (2013) suggest a propagating signal in sea level variability linked to atmospheric circulation and oceanic Kelvin waves, moving along the eastern boundary of the North Atlantic and into the Barents and Kara Seas, which is in line with the findings by Volkov et al. (2013) for the Barents Sea. The tide gauge-based studies agree that accounting for the effect of GIA constitutes a major source of uncertainty in the sea level rise estimates, in particular in the former location of the Fennoscandian ice sheet (Slangen et al. 2014) and thus the MOSJ region.

2.5.2 Monitoring Method

Currently, MOSJ includes observations of relative sea level (RSL), i.e. sea level relative to a coastal benchmark at the station, from tide gauges in Barentsburg, Tromsø, and Vardø. A further tide gauge in Svalbard is located in Ny-Ålesund. The tide gauge in Barentsburg is operated by Russian authorities. The Norwegian Mapping authority is responsible for the tide gauges in Ny-Ålesund and on mainland Norway. Data are available from the Permanent Service for Mean Sea Level (PSMSL, http://www.psmsl.org, Holgate et al. 2013). For this report, we use monthly and annual mean sea level data in the Revised Local Reference (RLR) version (PSMSL, 2017).

The tide gauge records have varying length (see Table 2), and several contain major gaps (see Fig. 12). While the gaps are relatively short for the time series from Tromsø and Barentsburg, the record in Vardø is interrupted between 1967-1983, and in Ny-Ålesund data are missing in the period 1988-1992.

To assess sea level changes from records of relative sea level, vertical land motion has to be taken into account. Various models exist to calculate the effect of GIA with rather large spread in estimated uplift velocities, but a full review is beyond the scope of this report. We therefore restrict ourselves to two versions of a global model (ICE_5G (VM2 L90), version 1.3, and ICE_6G_C (VM5a); Peltier et al. 2004; Peltier et al. 2015; Argus et al. 2014); a previous version of this model has also been used in Hansen (2010). Model data of present day rates for uplift were downloaded from http://www.atmosp.physics.utoronto.ca/~peltier/data.php. The Norwegian Mapping Authority provides

values at the position of the tide gauges on the Norwegian mainland on their website, these are included for comparison (data accessed at http://www.kartverket.no/en/sehavniva; for model details see Kierulf et al. 2014).

2.5.3 Current development

Fig. 12 shows monthly and annual mean sea level from the tide gauges included in MOSJ and from Ny-Ålesund. The time series display strong annual and semi-annual variability, and a 18.6 yr cycle related to the moon's nodal cycle. The 12-month running averages of the records from Vardø and Tromsø show a high degree of correlation (r=0.80), similarly, mean sea level at Ny-Ålesund and at Barentsburg are correlated, although not as clearly (r=0.50). Comparison of time series from mainland Norway and Svalbard does not reveal high correlation, even when taking into account potential lags. The gaps in the records limit however the reliability of such correlation analyses.

Trends in annual mean sea level were calculated using linear regression over the respective observation periods of the tide gauge records, and are given in Table 2. In Svalbard and Vardø, relative sea level is decreasing, whereas in Tromsø, no significant trend is observed. However, all trends depend strongly on the period chosen for the analysis, as was also stated in other studies using tide gauge data (e.g. Richter et al. 2012; Calafat et al. 2013; Simpson et al. 2015). The values here can therefore only be taken as approximation of the current development.

In a previous report (Hansen 2010) it was noted that the observations in Barentsburg might be compromised due to malfunctioning equipment. On PSMSL, it is stated that post 1995 Barentsburg data looks suspect. From visual inspection of the time series, we identified the period from 1995 to 2001 to behave notably different from the rest of the time series; we therefore recalculated the trend excluding data from these years. The resulting trend is less, but still pronounced with -2.32 mm/yr.

Quite remarkedly, while the trend in Barentsburg is less than reported in Hansen (2010), Ny-Ålesund is now experiencing a stronger decline in mean sea level. A continuing positive trend in GIA in Vardø partially offset the negative trend over the full observation period.

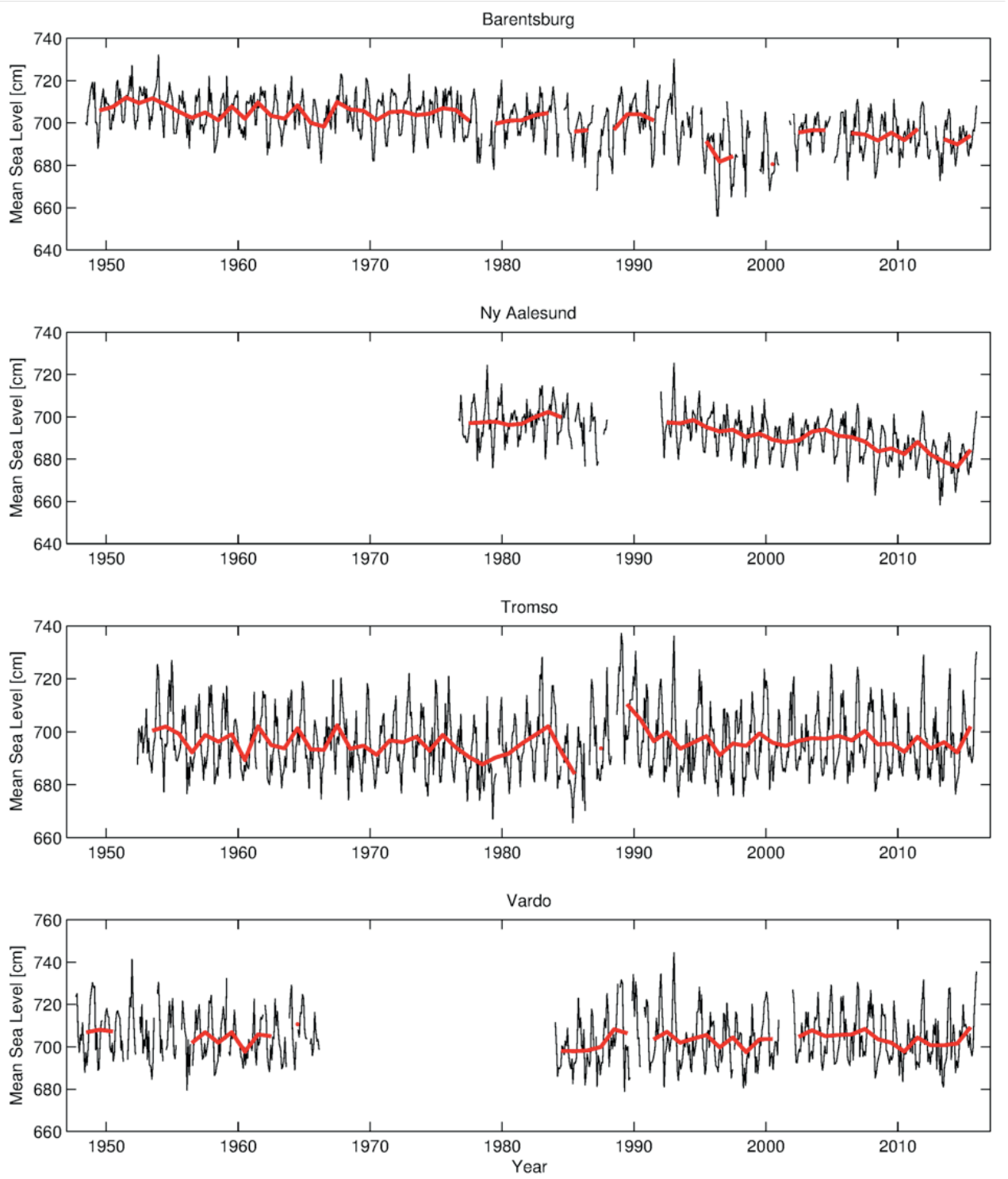

***Figure 12**: Relative mean sea level at Barentsburg, Ny-Ålesund, Tromsø, and Vardø (top to bottom). The black lines show monthly mean, the red lines annual mean sea level.*

***Table 2**: Trends in observed annual relative mean sea level and present day uplift rates at Barentsburg, Ny Ålesund, Tromsø, and Vardø.*

Tide gauge (PSMSL station ID)	Observation period	Trend observed [mm/yr]	GIA from ICE-5G [mm/yr]	GIA from ICE-6G_C [mm/yr]	GIA from the Norwegian Mapping Authority [mm/yr]
Barentsburg (#541)	1949 - 2015	-2.74	1.15	1.42	n/a
Ny Ålesund (#1421)	1977 - 2015	-4.75	0.48	0.70	n/a
Tromsø (#680)	1953 - 2015	0.01	1.30	0.70	2.6
Vardø (#524)	1948 - 2015	-0.32	1.45	0.87	2.7

For the tide gauges on the Norwegian mainland, the Norwegian Mapping Authority is providing estimates for the effect of GIA; the uplift rates for Tromsø and Vardø are given in Table 2. We also include model values for all locations. There is large spread between the different estimates, which demonstrates the uncertainties associated with estimations of vertical land movement, both due to GIA and other processes. While ICE_6G_C (VM5a) provides the most up-to-date global estimate of GIA, the Norwegian Mapping Authority model is likely more capable in capturing local effects. In particular in Svalbard, disappearance of land ice strongly influences the estimates (e.g. Omang & Kierulf 2011), whereas spatial variability and uncertainty in models of ice load during the last ice age influence GIA estimates (e.g. Richter et al. 2012; Kierulf et al. 2014; Auriac et al. 2016). Studies using GPS measurements can be used to constrain modelled uplift rates, however, GPS stations are often not co-located with tide gauges, or, as in the case of Barentsburg, entirely missing. Simpson et al. (2015) found uplift rates of 1 to 7 mm/yr from GPS stations across Norway; Omang & Kierulf (2011) and Mémin et al (2014) find similar values for Ny-Ålesund.

Taking into account these uplift rates, adjusted mean sea level trends (i.e. observed relative sea level plus uplift) are positive in all scenarios for Tromsø and Vardø. Using model rates, mean sea level in Svalbard is continuing to drop, albeit at a slower rate. GPS estimates of vertical land motion, however, are much larger than modeled values, and result in a sea level rise also in Svalbard.

2.5.4 Future predictions and projections; extremes

Church et al. (2013) state that it is very likely for global mean sea level to continue to rise at a rate that will exceed the rate observed for 1971-2010, i.e. the recently observed acceleration will continue. The rate is dependent on the development of future CO_2 emissions and other climate change drivers. As past sea level rise, future changes will display strong regional patterns, but only regions under the influence of current or former land ice and ice sheets might still experience sea level fall by the end of the 21st century. Increasing sea level will likely lead to increasing occurrence of extreme events, which might impact coastal structures, however, there is large uncertainty associated with regional projections and projections of extreme events (Church et al. 2013).

More recently, Carson et al. (2016) tried to further constrain regional deviations from global mean sea level rise, especially along coasts. They found significant difference between global and regional sea level changes by the end of the 21st century only for polar regions such as the Arctic and regions around

Greenland. Here, the effect of thermal expansion and input of mass from ice sheet melt might be offset by land uplift and smaller gravitational attraction due to reduced land ice mass on Greenland. For Norway and Svalbard, projections show lower than global average sea level rise, however, they are also among the regions with the largest uncertainties regarding the impact of GIA. Simpson et al. (2015) confirm that positive mean sea level rise can be expected for most of the Norwegian coast by the end of the century. Storm floods have larger effects in southern Norway than in western and northern Norway. There is generally little confidence in projections of strong winds and associated storm surges due to the low number of studies into future wind and wave climate and their findings of large uncertainties (Church et al. 2013). However, the current pattern of sea level rise along the Norwegian coast is expected to change little (Simpson et al. 2015).

2.5.5 Suggestions to MOSJ

Several of the tide gauge records used as indicators in MOSJ suffer from large gaps (Vardø) or uncertainty about data quality (Barentsburg). This could be addressed by including other available records in similar regions such as Hammerfest on mainland Norway, and Ny-Ålesund in Svalbard.

Simpson et al. (2015) provide an up-to-date overview of sea level along the Norwegian coast. In collaboration with the Norwegian Mapping Authority, a similar exercise for Svalbard and Jan Mayen could be done to improve knowledge about sea level changes and projections also in that region.

3 References

Aagaard, K., A. Foldvik, S.R. Hillman (1987): The West Spitsbergen Current: Disposition and water mass transformation. Journal of Geophysical Research, 92, 3778-3784.

AMAP - Arctic Monitoring and Assessment Programme - Arctic Ocean Acidification Assessments summary for policy makers (2013), Oslo, Norway.

Anderson, L., Chierici, G., Fogelqvist, E., Johannessen, T., 1999. Flux of anthropogenic and steady state carbon into the deep Greenland Sea. Journal of Geophysical Research.

Anderson L.G., Drange H., Chierici M., Fransson A., Johannessen T, Skjelvan I and Rey F. (2000). Annual carbon fluxes in the upper Greenland Sea based on measurements and a box model approach. 2000. Tellus, 52B, pp. 1013-1024.

Anderson L.G., E. Falck, E. P. Jones, S. Jutterstrom, J.H. Swift (2004): Enhanced uptake of atmospheric CO_2 during freezing of seawater: A field study in Storfjorden, Svalbard. Journal of Geophysical Research, 109, C06004, doi:10.1029/2003JC002120.

Argus, D.F., W. R. Peltier, R. Drummond, A. W. Moore (2014): The Antarctica component of postglacial rebound model ICE-6G_C (VM5a) based upon GPS positioning, exposure age dating of ice thicknesses, and relative sea level histories. Geophysical Journal International, 198(1), 537-563, doi:10.1093/gji/ggu140.

Auriac, A., P. L. Whitehouse, M. J. Bentley, H. Patton, J. M. Lloyd, A. Hubbard (2016): Glacial isostatic adjustment associated with the Barents Sea ice sheet: A modelling inter-comparison. Quaternary Science Reviews, 147, 122-135, doi:10.1016/j.quascirev.2016.02.011.

Bednaršek N., G. A. Tarling, D. C. E. Bakker, S. Fielding, E. M. Jones, H. J. Venables, P. Ward, A. Kuzirian, B. Lézé, R. A. Feely, E. J. Murphy (2012): Extensive dissolution of live pteropods in the Southern Ocean. Nature Geoscience, 5, doi: 10.1038/NGEO1635.

Bednaršek N, G. A. Tarling, D. C. E. Bakker, S. Fielding, R. A. Feely (2014): Dissolution dominating calcification process in polar pteropods close to the point of aragonite undersaturation. PLoS ONE 9(10): e109183. doi:10.1371/journal.pone.0109183.

Belkin, I. A., S. Levitus, J. Antonova, S.-A. Malmberg (1998): “Great Salinity Anomalies” in the North Atlantic. Progress in Oceanography, 41 1–68.

Beuchel F., B. Gulliksen, M. L. Carroll (2006): Long-term patterns of rocky bottom macrobenthic community structure in an Arctic fjord (Kongsfjorden, Svalbard) in relation to climate variability (1980- 2003). Journal of Marine Systems, 63(1/2), 35-48.

Berge J., G. Johnsen, F. Nilsen, B. Gulliksen, D. Slagstad (2005): Ocean temperature oscillations enable reappearance of blue mussels Mytilus edulis in Svalbard after a 1000 year absence. Marine ecology Progress Series, 303, 167-175.

Beszczynska-Möller, A., E. Fahrbach, U. Schauer, E. Hansen (2012): Variability in Atlantic water temperature and transport at the entrance to the Arctic Ocean, 1997–2010, ICES J. Mar. Sci., 69(5), 852–863.

Bourke, R.H., A.M. Wiegel, R.G. Paquette (1988): The westward turning branch of the West Spitsbergen Current. Journal of Geophysical Research, 93, 14065-14077.

Boyd, T.J., E.A. D'Asaro (1994): Cooling of the West Spitsbergen Current - wintertime observations west of Svalbard. Journal of Geophysical Research, 99, 22597-22618.

Calafat, F. M., D. P. Chambers, M. N. Tsimplis (2013): Inter-annual to decadal sea-level variability in the coastal zones of the Norwegian and Siberian Seas: The role of atmospheric forcing, J. Geophys. Res. Oceans, 118, 1287–1301, doi:10.1002/jgrc.20106.

Carroll, M. L., W. G. Ambrose, B. S. Levin, W. L. Locke, G. A. Henkes, H. Hop, P. E. Renaud (2011): Pan-Svalbard growth rate variability and environmental regulation in the Arctic bivalve Serripes groenlandicus. Journal of Marine Systems 88(2): 239-251.

Carson, M., A. Köhl, D. Stammer, A. B. A. Slangen, C. A. Katsman, R. S. W. van de Wal, J. Church, N. White (2016): Coastal sea level changes, observed and projected during the 20th and 21st century. Climatic Change, 134, 269-281, doi:10.1007/s10584-015-1520-1.

Chierici M., H. Drange, L. G. Anderson, T. Johannessen (1999) Inorganic carbon fluxes through the boundaries of the Greenland Sea Basin based on in situ observations and water transport estimates. Journal of Marine Systems 22 1999 295–309.

Chierici, M., A. Fransson, P. Dodd, M.A. Granskog, E. Hansen, (2013), Ocean Acidification state in Arctic outflow waters in the Fram Strait, abstract for Arctic Ocean Acidification Conference, 6-8th May, Bergen, Norway.

Chierici, M., A. Fransson., M.A. Granskog., P. Dodd., E. Hansen., C. Stedmon (2014): Ocean Acidification state in Arctic exchange waters – teleconnectivity, oral presentation at the Marine Day in Norway-Japanese Science symposium, 1-5th June, Tokyo, Japan, invited.

Church, J.A., P.U. Clark, A. Cazenave, J.M. Gregory, S. Jevrejeva, A. Levermann, M.A. Merrifield, G.A. Milne, R.S. Nerem, P.D. Nunn, A.J. Payne, W.T. Pfeffer, D. Stammer, A.S. Unnikrishnan (2013): Sea Level Change. In: Climate Change 2013: The Physical Science Basis. Contribution of Working Group I to the Fifth Assessment Report of the Intergovernmental Panel on Climate Change [Stocker, T.F., D. Qin, G.-K. Plattner, M. Tignor, S.K. Allen, J. Boschung, A. Nauels, Y. Xia, V. Bex and P.M. Midgley (eds.)]. Cambridge University Press, Cambridge, United Kingdom and New York, NY, USA.

Cokelet, E. D., N. Tervalon, J. G. Bellingham (2008): Hydrography of the West Spitsbergen Current, Svalbard Branch: Autumn 2001. J. Geophys. Res., 113, C01006, doi:10.1029/2007JC004150.

Cottier, F.R., V. Tverberg, M. E. Inall, H. Svendsen, F. Nilsen, C. Griffiths (2005): Water mass modification in an Arctic fjord through cross-shelf exchange: the seasonal hydrography of Kongsfjorden, Svalbard. J Geophys Res – Oceans 110, C12005.

Delworth, T. L., and M. E. Mann (2000), Observed and simulated multidecadal variability in the Northern Hemisphere, Clim. Dyn., 16(9), 661–676, doi: 10.1007/s003820000075

Fabry, V. J., B. A. Seibel, R. A. Feely, J. C. Orr (2008): Impacts of ocean acidification on marine fauna and ecosystem processes. ICES J Mar Sci, 65, 414–432, doi:10.1093/icesjms/fsn048.

Fauchald, P., P. Arneberg, J. Berge, S. Gerland, K. M. Kovacs, M. Reigstad, J. H. Sundet (2014): An assessment of MOSJ – The state of the marine environment around Svalbard and Jan Mayen. Norwegian Polar Institute Report Series No. 145, ISBN 978-82-7666-301-3, Tromsø, Norway.

Fetterer, F., K. Knowles, W. Meier, M. Savoie (2016): *Sea Ice Index, Version 2,* updated daily. Boulder, Colorado USA. NSIDC: National Snow and Ice Data Center. doi:10.7265/N5736NV7. [Accessed 28. April 2017].

Findlay, H.S., H. L. Wood, M. A. Kendall, J. I. Spicer, R. Twitchett, S. Widdicombe (2011): Comparing the impact of high CO2 on calcium carbonate structures in difference marine organisms. Mar Biol Res 7:565-575.

Fransson A, M. Chierici, H. Hop, H. Findlay, S. Kristiansen, A. Wold (2016): Late winter-to- summer change in ocean acidification state in Kongsfjorden, with implications for calcifying organisms. Polar Biol. 5 special issue on Kongsfjorden, 1-17, DOI:10.1007/s00300-016-1955.

Fransson, A., M. Chierici., D. Nomura, M. A. Granskog, S. Kristiansen, T. Martma, G. Nehrke (2015): Effect of glacial drainage water on the CO2 system and ocean acidification state in an Arctic tidewater-glacier fjord during two contrasting years. Journal of Geophysical Research- Oceans, 120, doi:10.1002/2014JC010320.

Fransson A., M. Chierici, L.A. Miller, G. Carnat, H. Thomas, E. Shadwick, S. Pineault, T.M. Papakyriakou (2013): Impact of sea ice processes on the carbonate system and ocean acidification state at the ice-water interface of the Amundsen Gulf, Arctic Ocean. Journal of Geophysical Research: Oceans, 118, 1–23, doi:10.1002/2013JC009164.

Furevik, T. (2001): Annual and interannual variability of Atlantic Water temperatures in the Norwegian and Barents Seas: 1980–1996. Deep Sea Research I, 48: 383–404.

Gerland, S., A. H. H. Renner (2007): Sea-ice mass-balance monitoring in an Arctic fjord. Annals of Glaciology, 46, 435-442.

Gerland, S., A. H. H. Renner, F. Godtliebsen, D. Divine, T. B. Løyning (2008): Decrease of sea ice thickness at Hopen, Barents Sea, during 1966-2007. Geophysical Research Letters, 35, L06501, doi:10.1029/2007GL032716.

Granskog, M., P. Assmy, S. Gerland, G. Spreen, H. Steen, and L. H. Smedsrud (2016), Arctic research on thin ice—Consequences of Arctic sea ice loss, Eos Trans. AGU, 97(5), 22–26, doi:10.1029/2016EO044097.

Hansen, J. R. (2010): Status og utviklingstrekk for klimaindikatorer i norsk del av Arktis; MOSJ tolkingsrapport – klima. Norwegian Polar Institute Report Series No. 130, ISBN 978-82-7666-263-4, Tromsø, Norway.

Hansen, E., S. Gerland, M. A. Granskog, O. Pavlova, A. H. H. Renner, J. Haapala, T. B. Løyning, and M. Tschudi (2013): Thinning of Arctic sea ice observed in Fram Strait: 1990–2011. J. Geophys. Res. Oceans, 118, 5202–5221, doi:10.1002/jgrc.20393.

Hansen, E., O.-C. Ekeberg, S. Gerland, O. Pavlova, G. Spreen, M. Tschudi (2014): Variability in categories of Arctic sea ice in Fram Strait. Journal of Geophysical Research, 119, 7175-7189, doi:10.1002/2014JC010048.
Hansen, E., S. Gerland, K. V. Høyland, O. Pavlova, G. Spreen (2015): Time variability in the annual cycle of sea ice thickness in the Transpolar Drift. Journal of Geophysical Research, 120, 8135-8150, doi:10.1002/2015JC011102.
Hattermann, T., P. E. Isachsen, W.-J. Von Appen, J. Albretsen, A. Sundfjord (2016): Eddy-driven recirculation of Atlantic Water in Fram Strait. Geophys.Res. Lett., 43, 3406–3414, doi:10.1002/2016GL068323.
Hátún, H., A. B. Sandø, H. Drange (2005): Influence of the Atlantic Subpolar Gyre on the thermohaline circulation. Science, 309: 1841–1844.
Haugan, P.M. (1999): Structure and heat content of the West Spitsbergen Current. Polar Research, 18, 183-188.
Henry, O., P. Prandi, W. Llovel, A. Cazenave, S. Jevrejeva, D. Stammer, B. Meyssignac, N. Koldunov (2012): Tide gauge-based sea level variations since 1950 along the Norwegian and Russian coasts of the Arctic Ocean: Contribution of the steric and mass components. Journal of Geophysical Research, 117, C06023, doi:10.1029/2011JC007706.
Herbaut, C., M.-N. Houssais, S. Close, A.-C. Blaizot (2015): Two wind-driven modes of winter sea ice variability in the Barents Sea. Deep-Sea Research I, 106, 97-115, doi:10.1016/j.dsr.2015.10.005.
Hindell MA, Lydersen C, Hop H, Kovacs KM (2012): Pre-partum diet of adult female bearded seals in years of contrasting ice conditions. PLoS ONE, 7(5): e38307 (10 pp.)
Holgate, S. J., A. Matthews, P. L. Woodworth, L. J. Rickards, M. E. Tamisiea, E. Bradshaw, P. R. Foden, K. M. Gordon, S. Jevrejeva, J. Pugh (2013): New Data Systems and Products at the Permanent Service for Mean Sea Level. Journal of Coastal Research: Volume 29, Issue 3: pp. 493 – 504. doi:10.2112/JCOASTRES-D-12-00175.1.
Holliday, N. P., Hughes, S. L., Bacon, S., Beszczynska-Moller, A., Hansen, B., Lavin, A., Loeng, H., et al. (2008): Reversal of the 1960s to 1990s freshening trend in the northeast North Atlantic and Nordic Seas. Geophysical Research Letters, 35: L03614, doi:10.1029/2007GL032675.
Hop, H., T. Pearson, E. N: Hegseth, K. M. Kovacs, C. Wiencke, C. Kwasniewski, S. Eiane, F. Mehlum, B. Gullriksen, et al. (2002): The marine ecosystem of Kongsfjorden, Svalbard. Polar Research, 21, 167-208.
Hop, H., S. Falk-Petersen, H. Svendsen, S. Kwasniewski, V. Pavlov, O. Pavlova, J. E. Søreide (2006): Physical and biological characteristics of the pelagic system across Fram Strait to Kongsfjorden. Progress in Oceanography, 71(2-4), 182-231,doi:10.1016/j.pocean.2006.09.007.
IPCC (2013): Climate Change 2013: The Physical Science Basis. Contribution of Working Group I to the Fifth Assessment Report of the Intergovernmental Panel on Climate Change [Stocker, T.F., D. Qin, G.-K. Plattner, M. Tignor, S.K. Allen, J. Boschung, A. Nauels, Y. Xia, V. Bex, P.M. Midgley (eds.)]. Cambridge University Press, Cambridge, United Kingdom and New York, NY, USA, 1535 pp.
Ingle, S. E (1975) Solubility of calcite in the ocean, Marine Chem., 3, 301–319.
Jeansson, E., S. Jutterström, B. Rudels, L. G. Anderson, K. A. Olsson, E. P. Jones, W. M. Smethie Jr., and J. H. Swift (2008), Sources to the East Greenland Current and its contribution to the Denmark Strait Overflow, Prog. Oceanogr., 78, 12–28, doi:10.1016/j.pocean.2007.08.031.
Jeansson, E., K. A. Olsson, T. Tanhua, and J. L. Bullister (2010), Nordic seas and Arctic Ocean CFC data in CARINA, Earth Syst. Sci. Data, 2, 79–97.
Jevrejeva, S., J. C. Moore, A. Grinsted, A. P. Metthews, G. Spada (2014): Trends and acceleration in global and regional sea levels since 1807. Global and Planetary Change, 113, 11-22, doi:10.1016/j.gloplacha.2013.12.004.
Jutterström, S., E. Jeansson, L. G. Anderson, R. Bellerby, E. P. Jones, W. M. Smethie Jr., and J. H. Swift (2008), Evaluation of anthropogenic carbon in the Nordic seas using observed relationships of N, P, and C versus CFCs, Prog. Oceanogr., 78, 78–84, doi:10.1016/j.pocean.2007.06.001.
Kaleschke, L., et al. (2016): SMOS sea ice product: Operational application and validation in the Barents Sea marginal ice zone. Remote Sensing of Environment, 180, 264-273, doi:10.1016/j.rse.2016.03.009.
Karcher, M. J., R. Gerdes, F. Kauker, C. Koberle (2003): Arctic warming: evolution and spreading of the 1990s warm event in the Nordic seas and the Arctic Ocean. Journal of Geophysical Research, 108(C2): 3034, doi:10.1029/2001JC001265.
Keck, A., J, Wiktor, R. Hapter, R. Nilsen (1999): Plankton assemblages related to physical gradients in an Arctic, glacier-fed fjord in summer. ICES J. Mar. Sci., 56, 203-214.
Kerr, R. A. 2000: A North Atlantic Climate Pacemaker for the Centuries. Science, 288(5473), doi: 10.1126/science.288.5473.1984

Kierulf, H. P., H. Steffen, M. J. R. Simpson, M. Lidberg, P. Wu, H. Wang (2014): A GPS velocity field for Fennoscandia and a consistent comparison to glacial isostatic adjustment models, J. Geophys. Res. Solid Earth, 119, 6613–6629, doi:10.1002/2013JB010889.

King, J., G. Spreen, S. Gerland, C. Haas, S. Hendricks, L. Kaleschke, C. Wang (2017): Sea-ice thickness from field measurements in the northwestern Barents Sea. J. Geophys. Res. Oceans, 122, 1497–1512, doi:10.1002/2016JC012199.

Krumpen, T., R. Gerdes, C. Haas, S. Hendricks, A. Herber, V. Selyuzhenok, L. Smedsrud, G. Spreen (2016): Recent summer sea ice thickness surveys in Fram Strait and associated ice volume fluxes. The Cryosphere, 10, 523-534, doi:10.5194/tc-10.523-2016.

Kruszewski, G. (2012): Ice condition in Hornsund and adjacent waters (Spitsbergen) during winter season 2010–2011. Problemy Klimatologii Polarnej, 22, 69–82.

Kwasniewski, S., et. al. (2012): Interannual changes in zooplankton on the West Spitsbergen Shelf in relation to hydrography and their consequences for the diet of planktivorous seabirds. ICES J. Mar. Sci., 69(5), 890-901, doi:10.1093/icesjms/fss076.

Kwok, R., G. Spreen, S. Pang (2013): Arctic sea ice circulation and drift speed: Decadal trends and ocean currents. Journal of Geophysical Research, 118, 2408-2425, doi:10.1002/jgrc.20191.

Lien, V. S., P. Schlichtholz, Ø. Skagseth, F. B. Vikebø (2017): Wind-driven Atlantic Water flow as direct mode for reduced Barents Sea ice cover. Journal of Climate, 30, 803-812, doi:10.1175/jcli-d-16-0025.1.

Limkilde Svendsen, P., O. B. Andersen, A. Aasbjerg Nielsen (2016): Stable reconstruction of Arctic sea level for the 1950–2010 period. J. Geophys. Res. Oceans, 121, 5697–5710, doi:10.1002/ 2016JC011685.

Manley, T.O. (1995): Branching of Atlantic Water within the Greenland-Spitsbergen passage: An estimate of recirculation. Journal of Geophysical Research, 100, 20627-20634.

Manno, C. et al. (2017): Shelled pteropods in peril: assessing vulnerability in a high CO_2 ocean. Earth Science Review, doi:10.1016/j.earscirev.2017.04.005.

Marnela, M., B. Rudels, M. N. Houssais, A. Beszczynska-Möller, P. B. Eriksson (2013): Recirculation in the Fram Strait and transports of water in and north of the Fram Strait derived from CTD data. Ocean Sci., 9(3), 499–519.

Meier, W. N., et al. (2014): Arctic sea ice in transformation: A review of recent observed changes and impacts on biology and human activity. Rev. Geophys., 51, doi:10.1002/2013RG000431.

Mémin, A., G. Spada, J-.P. Boy, Y. Rogister, J. Hinderer (2014): Decadal geodetic variations in Ny-Ålesund (Svalbard): role of past and present ice-mass changes. Geophys J Int, 198 (1): 285-297. doi: 10.1093/gji/ggu134.

Mucci, A.: The solubility of calcite and aragonite in seawater at various salinities, temperatures and at one atmosphere pressure (1983), Am. J. Sci., 283, 781–799.

Muckenhuber, S., F. Nilsen, A. Korosov, S. Sandven (2016): Sea ice cover in Isfjorden and Hornsund, Svalbard (2000–2014) from remote sensing data, The Cryosphere, 10, 149-158, doi:10.5194/tc-10-149-2016.

NOAA, 2017: AMO (Atlantic Multidecadal Oscillation) Index, Climate Timeseries calculated at NOAA PSD. Obtained from https://www.esrl.noaa.gov/psd/data/timeseries/AMO.

Nondal, G., R. G. J. Bellerby, A. Olsen, T. Johannessen, and J. Olafsson (2009), Optimal evaluation of the surface ocean CO2 system in the northern North Atlantic using data from Voluntary Observing Ships, Limnol. Oceanogr. Methods, 7, 109–118.

Norwegian Polar Institute, 2017: The Fram Strait Arctic Outflow Observatory. Research Project. http://www.npolar.no/en/projects/fram-strait-arctic-outflow-observatory.html

Olsen, A., R. G. J. Bellerby, T. Johannessen, A. M. Omar, and I. Skjelvan (2003), Interannnual variability in the wintertime air-sea flux of carbon dioxide in the northern North Atlantic, 1981–2001, Deep Sea Res. Part I, 50, 1323–1338, doi:10.1016/S0967-0637(03)00144-4.

Olsen A., A. M. Omar, R. G. J. Bellerby, T. Johannessen, U. Ninnemann, K. R. Brown, K. A. Olsson, J. Olafsson, G. Nondal, C. Kivimäe, S. Kringstad, C. Neill, S. Olafsdottir (2006): Magnitude and origin of the anthropogenic CO2 increase and 13C Suess effect in the Nordic seas since 1981. Global Biogeochem Cycles 20, GB3027, doi:10.1029/2005GB002669.

Olsen, A. (2009), Nordic seas total dissolved inorganic carbon data in CARINA, Earth Syst. Sci. Data, 1, 35–43.

Olsen A., A. M. Omar, E. Jeansson, L. G. Anderson, R. G. J. Bellerby (2010) Nordic seas transit time distributions and anthropogenic CO2. JGR, 115, C5 doi: 10.1029/2009JC005488.

Omang, O. C. D., H. P. Kierulf (2011): Past and present-day ice mass variation on Svalbard revealed by

superconducting gravimeter and GPS measurements. Geophys. Res. Lett., 38, L22304, doi:10.1029/2011GL049266.
Onarheim, I. H., L. H. Smedsrud, R. B. Ingvaldsen, F. Nilsen (2014): Loss of sea ice during winter north of Svalbard. Tellus A, 66, 23933, doi:10.3402/tellusa.v66.23933.
O'Reilly, C. H., M. Huber, T. Woollings, and L. Zanna, 2016: The signature of low-frequency oceanic forcing in the Atlantic Multidecadal Oscillation, Geophys. Res. Lett., 43, 2810–2818, doi:10.1002/2016GL067925.
Overland, J.E. (2016): Is the melting Arctic changing midlatitude weather? Phys. Today 69 (3), p. 38, doi:10.1063/PT.3.3107.
Patton, H., A. Hubbard, K. Andreassen, A. Auriac, P. L. Whitehouse, A. P. Stroeven, C. Shackleton, M. Winsborrow, J. Heyman, A. M. Hall (2017): Deglaciation of the Eurasian ice sheet complex. Quaternary Science Reviews, 169, 148-172, doi:10.1016/j.quascirev.2017.05.019.
Pavlova, O., V. Pavlov, S. Gerland (2014): The impact of winds and sea surface temperatures on the Barents Sea ice extent, a statistical approach. Journal of Marine Systems, 130, 248-255, doi:10.1016/j.jmarsys.2013.02.011.
Peltier, W. R. (2004): Global Glacial Isostasy and the Surface of the Ice-Age Earth: The ICE-5G (VM2) Model and GRACE, Ann. Rev. Earth and Planet. Sci., 32, 111-149.
Peltier, W.R., Argus, D.F., Drummond, R. (2015): Space geodesy constrains ice-age terminal deglaciation: The global ICE-6G_C (VM5a) model. J. Geophys. Res. Solid Earth, 120, 450-487, doi:10.1002/2014JB011176.
Permanent Service for Mean Sea Level (PSMSL) (2017): Tide Gauge Data. Retrieved 16 Apr 2017 from http://www.psmsl.org/data/obtaining/.
Piechura J., W. Walczowski (2009): Warming of the West Spitsbergen Current and sea ice north of Svalbard. OCEANOLOGIA, 51 (2). pp. 147–164.
Piquet A.M.-T., W. H. van de Poll, R. J. W. Visser, C. Wiencke, H. Bolhuis, A. G. J. Buma (2014): Springtime phytoplankton dynamics in Arctic Krossfjorden and Kongsfjorden (Spitsbergen) as a function of glacier proximity. Biogeosciences 11:2263–2279, doi:10.5194/bg-11-2263-2014.
Polyakov, I. V., A. Beszczynska, E. C. Carmack, I. A. Dmitrenko, E. Fahrbach, I. E. Frolov, R. Gerdes, et al. (2005): One more step toward a warmer Arctic. Geophysical Research Letters, 32: L17605, doi:10.1029/2005GL023740.
Polyakov, I. V., V. A. Alexeev, U. S. Bhatt, E. I. Polyakova, X. Zhang (2010): North Atlantic warming: patterns of long-term trend and multidecadal variability. Clim. Dyn. 34:439–457, doi:10.1007/s00382-008-0522-3.
Renner, A. H. H., S. Hendricks, S. Gerland, J. Beckers, C. Haas, T. Krumpen (2013): Large-scale ice thickness distribution of first-year sea ice in spring and summer north of Svalbard. Annals of Glaciology, 54(62), 13-18, doi:10.3189/2013AoG62A146.
Renner, A. H. H., S. Gerland, C. Haas, G. Spreen, J. F. Beckers, E. Hansen, M. Nicolaus, H. Goodwin (2014): Evidence of Arctic sea ice thin- ning from direct observations, *Geophys. Res. Lett.*, *41*, 5029–5036, doi:10.1002/2014GL060369.
Richter, K., J. E. Ø. Nilsen, H. Drange (2012): Contributions to sea level variability along the Norwegian coast for 1960–2010, J. Geophys. Res., 117, C05038, doi:10.1029/2011JC007826.
Ries, J.B. (2012): Oceanography: A sea butterfly flaps its wings. Nat Geosci, 5:845-846.
Rudels, B., M. Korhonen, U. Schauer, S. Pisarev, B. Rabe, A. Wisotzki (2015): Circulation and transformation of Atlantic water in the Eurasian Basin and the contribution of the Fram Strait inflow branch to the Arctic Ocean heat budget. Prog. Oceanogr. 132, 128—152, doi:10.1016/j.pocean.2014.04.003.
Sabine, C. L., R. A. Feely, N. Gruber, R. M. Key, K. Lee, J. L. Bullister, R. Wanninkhof, C. S. Wong, D. W. R. Wallace, B. Tilbrook, F. J. Millero, T. H. Peng, A. Kozyr, T. Ono, A. F. Rios (2004) The Oceanic Sink for Anthropogenic CO2. Science 305:367-371, doi: 10.1126/science.1097403.
Saloranta, T.M., H. Svendsen (2001): Across the Arctic front west of Spitsbergen: high-resolution CTD sections from 1998-2000. Polar Research, 20, 177-184.
Schauer, U., H. Loeng, B. Rudels, V. K. Ozhigin, W. Dieck (2002): Atlantic Water flow through the Barents and Kara Seas. Deep Sea Research I, 49: 2281–2298.
Simpson, M. J. R., J. E. Ø. Nilsen, O. R. Ravndal, K. Breili, H. Sande, H. P. Kierulf, H. Steffen, E. Jansen, M. Carson, O. Vestøl (2015): Sea Level Change for Norway: Past and Present Observations and Projections to 2100. Norwegian Centre for Climate Services report 1/2015, ISSN 2387-3027, Oslo, Norway.
Skjelvan, I., Johannessen, T., Miller, L., (1999). Interannual variability of fCO2 in the Greenland and Norwegian Seas, Tellus.

Skogen M.D., A. Olsen, K. Y. Børsheim, A. B. Sandø, I. Skjelvan (2014): Modelling ocean acidification in the Nordic and Barents Seas in present and future climate. Journal of Marine Systems, 131, 10-20.

Slangen, A. B. A., R. S. W. van de Wal, Y. Wada, L. L. A. Vermeersen (2014): Comparing tide gauge observations to regional patterns of sea-level change (1961-2003). Earth System Dynamics, 5, 243-255, doi:10.5194/esd-5-243-2014.

Smedsrud, L. H., A. Sirevaag, K. Kloster, A. Sorteberg, S. Sandven (2001): Recent wind driven high sea ice area export in the Fram Strait contributes to Arctic sea ice decline. The Cryosphere, 5, 821-829, doi:10.5194/tc-5-821-2011.

Smedsrud, L. H., M. H. Halvorsen, J. C. Stroeve, R. Zhang, K. Kloster (2017): Fram Strait sea ice export variability and September Arctic sea ice extent over the last 80 years. The Cryosphere, 11, 65-79, doi:10.5194/tc-11-65-2017.

Spielhagen, R. F., K. Werner, S. Å. Sørensen, K. Zamelczyk, E. Kandiano, G. Budeus, K. Husum, T. M. Marchitto, M. Hald (2011): Enhanced modern heat transfer to the Arctic by warm Atlantic water. Science 331(6016): 450-3

Spreen, G., S. Kern, D. Stammer, E. Hansen (2009): Fram Strait sea ice volume export estimated between 2003 and 2008 from satellite data. Geophysical Research Letters, 36, L19502, doi:10.1029/2009GL039591.

Svendsen H, A. Beszczynska-Møller, J. O. Hagen, B. Lefauconnier, V. Tverberg, et al. (2002): The physical environment of Kongsfjorden-Krossfjorden, an Arctic fjord system in Svalbard. Polar Research, 21, 133–166.

Volkov, D. L., F. W. Landerer, S. A. Kirillov (2013): The genesis of sea level variability in the Barents Sea. Continental Shelf Research, 66, 92-104, doi:10.1016/j.csr.2013.07.007.

Walczowski W., J. Piechura (2011): Influence of the West Spitsbergen Current on the local climate. Int. J. Climatol. 31: 1088–1093, doi:10.1002/joc.2338.

Zhang, R. (2017), On the persistence and coherence of subpolar sea surface temperature and salinity anomalies associated with the Atlantic multidecadal variability, Geophys. Res. Lett., 44, 7865–7875, doi:10.1002/2017GL074342

Zhuravskiy, D., B. Ivanov, A. Pavlov (2012): Ice conditions at Gronfjorden Bay, Svalbard, from 1974 to 2008, Polar Geogr., 35, 169– 176, doi:10.1080/1088937X.2012.662535.

Miljømerket trykksak 2041 0699 | Trykk: Bodoni

048 KORTRAPPORT / BRIEF REPORT
NORSK POLARINSTITUTT / NORWEGIAN POLAR INSTITUTE 2018